Environment International 176 (2023) 107961

Contents lists available at ScienceDirect

Environment International

journal homepage: www.elsevier.com/locate/envint

Full length article

Spatiotemporal variations of tropospheric ozone in Spain (2008–2019)

Jordi Massagué [a,b,*], Miguel Escudero [c], Andrés Alastuey [a], Enrique Mantilla [d], Eliseo Monfort [e], Gotzon Gangoiti [f], Carlos Pérez García-Pando [g,h], Xavier Querol [a]

[a] Institute of Environmental Assessment and Water Research (IDAEA-CSIC), 08034 Barcelona, Spain
[b] Department of Mining, Industrial and ICT Engineering, Universitat Politècnica de Catalunya - BarcelonaTech, UPC, 08242 Manresa, Spain
[c] Department of Applied Physics, School of Engineering and Architecture, Universidad de Zaragoza, 50018 Zaragoza, Spain
[d] Mediterranean Center for Environmental Studies, CEAM, Valencia 46980, Spain
[e] Institute of Ceramic Technology (ITC), Universitat Jaume I, 12006 Castellón, Spain
[f] Faculty of Engineering, University of the Basque Country UPV/EHU, 48013 Bilbao, Spain
[g] Barcelona Supercomputing Center, 08034 Barcelona, Spain
[h] ICREA, Catalan Institution for Research and Advanced Studies, 08010 Barcelona, Spain

ARTICLE INFO

Handling Editor: Marti Nadal

Keywords:
Tropospheric ozone concentration distribution
Trends
Mann-Kendall Theil-Sen test
Air quality and pollution
Human and vegetation exposure O3 metrics

ABSTRACT

This study aims to support the development of Spain's Ozone Mitigation Plan by evaluating the present-day spatial variation (2015–2019) and trends (2008–2019) for seven ground-level ozone (O_3) metrics relevant for human/ecosystems exposure and regulatory purposes.

Results indicate that the spatial variation of O_3 depends on the part of the O_3 distribution being analyzed. Metrics associated with moderate O_3 concentrations depict an increasing O_3 gradient between the northern and Mediterranean coasts due to climatic factors, while for metrics considering the upper end of the O_3 distribution, this climatic gradient tends to attenuate in favor of hotspot regions pointing to relevant local/regional O_3 formation. A classification of atmospheric regions in Spain is proposed based on their O_3 pollution patterns, to identify priority areas (or O_3 hotspots) where local/regional precursor abatement might significantly reduce O_3 during pollution episodes.

The trends assessment reveals a narrowing of the O_3 distribution at the national level, with metrics influenced by lower concentrations tending to increase over time, and those reflecting the higher end of the O_3 distribution tending to decrease. While most stations show no statistically significant variations, contrasting O_3 trends are evident among the O_3 hotspots. The Madrid area exhibits the majority of upward trends across all metrics, frequently with the highest increasing rates, implying increasing O_3 associated with both chronic and episodic exposure. The Valencian Community area exhibits a mixed variation pattern, with moderate to high O_3 metrics increasing and peak metrics decreasing, while O_3 in areas downwind of Barcelona, the Guadalquivir Valley and Puertollano shows no variations. Sevilla is the only large Spanish city with generalized O_3 decreasing trends.

The different O_3 trends among hotspots highlight the need for mitigation measures to be designed at a local/regional scale to be effective. This approach may offer valuable insights for other countries developing O_3 mitigation plans.

1. Introduction

Tropospheric ozone (O_3) is a key air pollutant that harms human health and the environment and is an important greenhouse gas in terms of radiative forcing (WHO, 2006, 2013a, b; Fowler et al., 2009; Myhre et al., 2013; GBD, 2016; IPCC, 2021). Epidemiological studies have indicated an impact on human morbidity and mortality from both episodic and long-term exposure to O_3. This compound is secondary, 90% of which, globally, arises from photochemical reactions in precursors, particularly nitrogen oxides (NOx), non-methane volatile organic compounds (VOCs), methane (CH_4), and carbon monoxide (CO), and the rest from stratospheric contributions (McLinden et al., 2000; Olson et al., 2001; Stevenson et al., 2006; Young et al., 2013).

European Directive 2008/50/EC on air quality (EC, 2008) defines O_3 thresholds for the protection of human health with respect to: (i) a target value (TV), set at 120 $\mu g \cdot m^{-3}$ for a maximum daily 8-h average (MDA8)

* Corresponding author.
E-mail address: jordi.massague@idaea.csic.es (J. Massagué).

https://doi.org/10.1016/j.envint.2023.107961
Received 8 February 2023; Received in revised form 5 April 2023; Accepted 3 May 2023
Available online 8 May 2023

concentration, not to be exceeded on more than 25 days per year, averaged over 3 years, and a long-term objective (LTO)—not yet in force—for which the same threshold should not be exceeded; (ii) information (IT) and alert thresholds of maximum hourly concentrations of 180 and 240 $\mu g \cdot m^{-3}$, respectively. The WHO guideline levels (AQG) provide two more-severe thresholds: 100 $\mu g \cdot m^{-3}$ for the MDA8, never to be exceeded, and 60 $\mu g \cdot m^{-3}$ as an average of the 6 months with the highest annual O_3 concentrations (WHO, 2021). For the protection of vegetation, the Directive uses the AOT40 metric—an annual sum of the excess of hourly concentrations over 80 $\mu g \cdot m^{-3}$ (40 ppb) during daylight hours, calculated from May to July.

Nearly all (99%) of the urban European population is exposed to O_3 levels exceeding the WHO AQG and 96% of the agricultural areas are exposed to O_3 above the LTO set by the Directive for the protection of vegetation (EEA, 2020). The Southern European regions, and especially the Mediterranean Basin, are the most exposed to O_3 pollution in Europe, where Spain and other countries systematically exceed the LTOs and TVs for the protection of health and vegetation (EEA, 2021).

In Spain, the phenomenology of O_3 is highly complex, as many factors may influence O_3 high concentrations (e.g., Millán et al., 1997, 2000; Dieguez et al., 2009; Dieguez et al., 2014; Gangoiti et al., 2001; Millán, 2014), including: (i) characteristic climatic, topographic, and meteorological patterns; (ii) high biogenic emissions during the warm seasons (Seco et al., 2011); (iii) *meso*-meteorological circulations that develop during summer in the absence of strong synoptic advections in certain areas (Querol et al., 2016, 2017, 2018); (iv) regional transport of O_3 (Pay et al., 2019); (v) high emissions of precursors in specific atmospheric basins (Querol et al., 2017, 2018; Escudero et al., 2019); and (vi) stratospheric intrusions (Kalabokas et al., 2017).

O_3 trends in Spain have been previously studied at a national scale (Dieguez et al., 2014; Querol et al., 2014, 2016; Santurtún et al., 2015) or larger-scale multi-country studies (e.g., Sicard et al., 2013; Sicard et al., 2018; Fleming et al., 2018; EEA, 2020). It should be considered that the aggregation of data from several air quality monitoring stations (AQMSs) into a single trend can mask the variability across the network (Colette et al., 2016). Also, O_3 trend analyses may lead to different conclusions depending on (i) the type of AQMS considered, for example, in a same time period, urban AQMSs may tend to record positive O_3 trends, while rural stations downwind of emission sources may record O_3 negative trends (e.g. Sicard et al., 2013); (ii) the time period considered, as meteorology or changes in precursors emissions may influence O_3 trends, for example, Querol et al. (2016), found that the severe 2003 European heat wave had a major influence on the 2000–2015 O_3 trends in Spain; (iii) the specific O_3 metrics assessed, because the same time series may show opposite trends depending on which part of the O_3 distribution is considered (e.g. Lefohn et al., 2017, 2018; Yan et al. 2019; Sicard, 2021).

To our knowledge, there are no updated studies of O_3 spatiotemporal variations in Spain. Within the framework of the implementation of a national Ozone Mitigation Plan, this study aims to support the design of emission reduction policies adapted to the different regions in the country. Thus, by including and individually assessing all the types of AQMSs available in Spain, and considering several relevant O_3 metrics, the present study is intended to (i) evaluate the current O_3 spatial variations, (ii) identify and classify atmospheric regions in Spain regarding their O_3 phenomenology, a type of analysis that is crucial for the establishment of effective policies, and (iii) analyze how O_3 levels in the different regions have varied over time.

The chosen period (2008–2019) for the assessment of O_3 trends is framed between two events that strongly influenced the emissions of O_3 precursors globally—the global financial crisis that began in 2008 and the COVID-19 outbreak in 2020 (Castellanos and Boersma, 2012; Querol et al., 2014; Sokhi et al., 2021). Thus, we consider the selected period to be relevant for the assessment of current policy actions and is long enough to perform robust short-term O_3 trend assessments (Monks et al., 2015).

2. Methodology

2.1. Study area

This study is focused in mainland Spain and the Balearic Islands (Fig. 1a). The location and type of the AQMSs used are shown in Fig. 1b, the selection criteria of which are justified below. Table S1 (supplemental) provides detailed information on each AQMS, and Figure S1.1 provides information on land cover and use, demographics, and main climatic characteristics of the area of study. Spain is the most densely populated country in Europe in terms of the built-up-area population density (Batista e Silva et al., 2021), where Madrid, Barcelona, Valencia and Sevilla are the most populated metropolitan areas (Fig. S1.1a).

The prevailing meteorological conditions produce a clear positive north–south gradation (Fig. S1.1c–f). In the northern and north-western areas, O_3 concentrations tend to be the lowest due to unfavorable conditions for O_3 production (Gangoiti et al., 2002, 2006; Saavedra et al., 2012). In contrast, in central, southern and Mediterranean areas, O_3 concentrations are higher due to the large precursor emissions, the predominant meteorological conditions during warm seasons, and the characteristic orography that enhances O_3 formation and accumulation (Millán et al., 1997, 2000; Gangoiti et al., 2001).

The areas in Spain that are frequently affected by the most intense O_3 episodes were identified by Dieguez et al. (2009) and Querol et al. (2016), and are highlighted in light green in Fig. 1a. The O_3 phenomenology in such areas has been studied previously—the Madrid metropolitan area (e.g., Plaza et al., 1997; Querol et al., 2018; Reche et al., 2018; Escudero et al., 2019), northern Barcelona (e.g., Querol et al., 2017; Massagué et al., 2019), the Guadalquivir Valley (e.g., Notario et al., 2012; in 't Veld et al., 2021; Massagué et al., 2021), the Valencian Community, generally including the O_3 dynamics affecting the Western Mediterranean (e.g., Millán et al., 1997, 2000; Gangoiti et al., 2001), and the Puertollano Basin (e.g., Saiz-Lopez et al., 2009; Notario et al., 2013).

2.2. Data

2.2.1. Ground-level measurements

We used O_3, hourly data series from all the AQMSs in Spain that (i) reported data to the European Council (EC) in the period (according to Decision 2011/850/UE), (ii) were active at least one of the last two years in the period (2018 or 2019), and (iii) fulfilled the selection criteria described below.

For the AQMS, we used the classification used in Europe for fixed sampling points (EC, 2004; 2008; 2011), based on the environment represented by each station and the predominant emission sources, shown in brackets, i.e., rural (industrial, background or regional background), suburban (traffic, industrial or background) or urban (traffic, industrial or background). Among the rural regional background sites, 13 AMQSs belong to the European Monitoring and Evaluation Program (EMEP) network. We further justify the need to consider all types of AQMSs in Spain, since, as some authors indicated, the classification used for primary pollutants is not always the most appropriate for O_3 (Millán et al., 2000; Escudero et al., 2014; Tapia et al., 2016; Querol et al., 2016, 2017, 2018). Section S2 (supplemental) describes data processing and screening methods. We considered years with valid data to be those with at least 75% of the records available, (e.g, Fleming et al., 2018; Lefohn et al., 2018) and applied this data-capture threshold to all averaging levels.

The trend estimations covered a 12-year period (2008–2019), with each AQMS required to have at least 10 years' worth of valid data—a period long enough to estimate short-term O_3 trends (Monks et al., 2015). As in e.g. Fleming et al. (2018), the present-day distribution assessment covered the last 5 years of the period used for trends (thus, 2015–2019), with each AQMS required to have at least 3 years' worth of valid data for that period (e.g., Schultz et al., 2017).

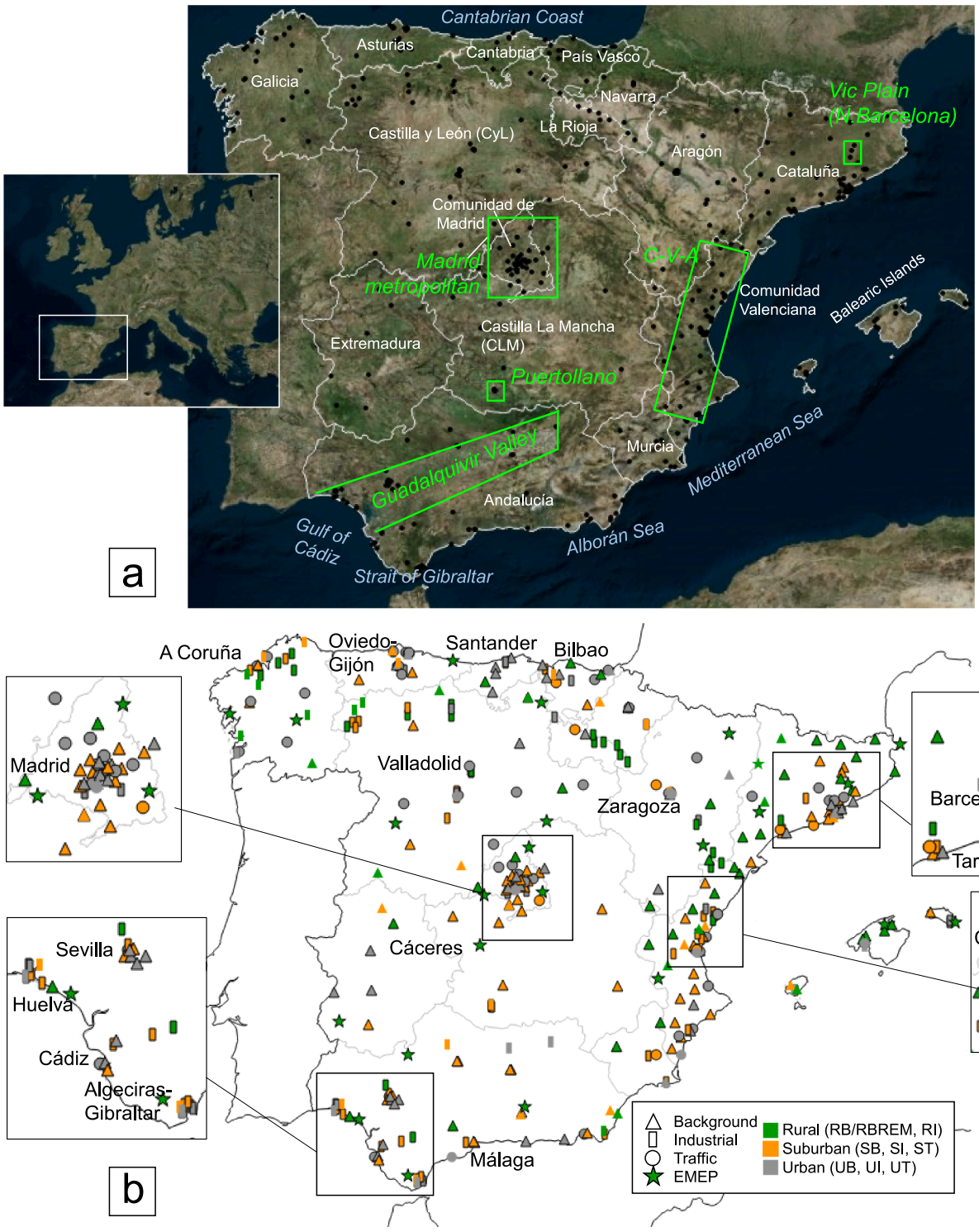

Fig. 1. (a) Autonomous regions in Spain—white; high O_3 areas (fully described in Querol et al., 2016) relevant to this study—light green; C-V-A—Castellón, Valencia, and Alicante; CyL—Castilla y León; CLM—Castilla–La Mancha. Black points in (a)—AQMSs referred to in (b). (b) AQMSs by type of area (different colors for rural, suburban, and urban) and type of station (different shapes for traffic, industrial, and background). UT/UI/UB—urban (traffic/industrial/background); ST/SI/SB—suburban (traffic/industrial/background); and RB/RI/RBREM—rural (background/industrial/regional background). Symbols with black edges—stations used for trend and present-day assessments; without edges—stations used only for present-day assessments. (For interpretation of the references to colour in this figure legend, the reader is referred to the web version of this article.)

The 12-year period used for the trends assessment, is between two major events that profoundly changed emissions on a global scale, i.e. the global crisis in 2008 and the COVID-19 pandemic in 2020. In Spain, these two events had a marked effect on the O_3 concentrations, see Section S3 (supplemental). For the design of current emission reduction policies, we are therefore interested in studying the period 2008–2019.

Hence, to robustly estimate trends, we used annual values of the metrics from each AQMS, using the non-parametric Mann–Kendall test along with the Theil–Sen statistical estimator (hereafter, MK–TS) (Theil, 1950; Sen, 1968), as used in Colette et al. (2016), Fleming et al. (2018),

Lefohn et al. (2018), among others. To this end, we used the R package Openair (Carslaw and Ropkins, 2012; R Core Team, 2021) to obtain the regression parameters (slope, uncertainty, and p-value), estimated via bootstrap resampling. We considered the trends to be statistically significant if $p < 0.05$, as used in all the references in the extensive review by Sicard (2021). Hereafter, we refer to each statistically significant trend simply as 'trend', unless otherwise specified.

Based on these data availability constraints and inspections, we used data from 364 and 304 AQMSs for the present-day and trend assessments, respectively. The number of stations with available data is different depending on the metric considered (see detailed information in Tables S1.1 to S1.3).

The concentrations are expressed in micrograms per cubic meter, as in the Directive 2008/50/EC. A conversion factor of 1 $\mu g \cdot m^{-3} = 0.5$ ppb at a reference temperature of 20 °C and 1 atmosphere of standard pressure can be used (Fleming et al., 2018).

2.2.2. O_3 metrics

Different conclusions can be drawn when assessing emission control strategies, depending on the specific metrics used. Thus, it is necessary to consider O_3 metrics across the O_3 distribution rather than solely focusing on the mid-range levels, such as mean/median concentrations (Lefohn et al., 2017; 2018). To this end, we used some relevant O_3 metrics, focusing on a wide part of the O_3 distribution, i.e. metrics influenced by moderate, high and peak O_3 concentrations (Table 1).

For reference, we included assessments on two additional metrics in Section S1 (supplemental): O3AS, which measures April-September mean O_3 concentrations, and EU60, which measures the annual sum of days with MDA8 > 120 $\mu g \cdot m^{-3}$, equivalent to the number of exceedances of the Directive's LTO (used e.g. in Colette et al., 2016).

2.2.3. Meteorological parameters

To complement the analyses, we used the fifth iteration of the ECMWF global reanalysis (ERA5) to obtain georeferenced monthly averaged meteorological data. Although ERA5 only provides a modeled approximation of atmospheric conditions, it is a continuous dataset in time and space, with regular 0.25°×0.25° spatial resolution (Hersbach et al., 2019). We examined nine meteorological parameters that can impact surface O_3 (Jacob and Winner, 2009; Coates et al., 2016; Lefohn et al., 2018; Otero et al., 2016; von Schneidemesser et al., 2015; Wei et al., 2022), including temperature, surface solar radiation downwards, downward UV radiation at the surface, cloud cover, boundary layer height, evaporation, surface wind speed, surface pressure, and total precipitation (refer to Section S2 for calculation details). We computed the annual April-September averages for each grid pixel to determine the present-day (2015–2019) spatial variability.

3. Results and discussion

For each metric analyzed, the below figures in Section 3.1 show the results of both present-day and trends assessments together. As for the discussion, in Section 3.1 we first discuss the present-day assessment, in Section 3.2 we present the classification of regions according to the O_3 behavior, and in Section 3.3, the trends assessment.

3.1. Present-day spatial variation (2015–2019)

The metric used here for the assessment of mid-range O_3 levels was the annual O_3 mean concentrations (O3YR, see Fig. 2). A clear gradient was evident between the Cantabrian and the Mediterranean coasts (Fig. 2a, b), with the northern third of the country having the lowest O_3 concentrations (28–50 $\mu g \cdot m^{-3}$, 23% of the AQMSs), mainly because of meteorological conditions that do not favor O_3 production (Gangoiti et al., 2002, 2006; Saavedra et al., 2012), and the minima being recorded in urban and/or well-industrialized areas where the ozonolysis of VOCs and titration by NO consume a lot of the O_3 (e.g., Solberg et al., 2005).

Very few AQMSs (3%) recorded such low concentrations in the central and southern half of the country, and mostly these were in high-traffic locations in Madrid, Valencia, and Sevilla. Conversely, high O3YR concentrations (>78 $\mu g \cdot m^{-3}$, 5% of the AQMSs) were mostly recorded by rural background/regional AQMSs, as expected (Wilson et al., 2012), and those located in/around Madrid, Andalucía, Cataluña, Valencian Community, and the Balearic Islands. The only non-rural background/regional AQMSs recording these high O_3 concentrations were found in Andalucía (suburban/rural industrial types), and at the border between

Table 1
O_3 metrics for present-day (2015–2019) and trend (2008–2019) assessments. The first five metrics are used for human health exposure to O_3 and ordered according to the part of the O_3 distribution of concentrations on which they focus. Thus, the first metric is associated to the lowest concentrations (O3YR), and the part of the O_3 distribution considered grows progressively up to the fifth metric, which is associated with the highest concentrations (IT90, number of exceedances of the Information Threshold (Directive 2008/50/EC). The last two metrics are used for vegetation exposure to O_3. *The Target Value (TV), Directive 2008/50/EC) sets a maximum of 25 days with maximum daily 8-hour mean concentrations (MDA8) > 120 $\mu g \cdot m^{-3}$, averaged over 3 years (EC, 2008). Our assessment used 5-year averages, which do not strictly represent legal exceedances of the TV, but rather indicate relevant potential exceedances.

	O_3 metric (units)	Definition	Assessment objective	Aggregation period	Example reference
Mean O_3 levels	O3YR ($\mu g \cdot m^{-3}$)	Annual mean concentration	Mid O_3 levels Global baseline at RB sites (HTAP, 2010). Close to emission sources can be influenced by night and/or winter O_3 titration (Sicard et al., 2013; Colette et al., 2016)	Annual	Sicard et al. (2016)
Human health (mid-high O_3 levels)	SOMO35 ($\mu g \cdot m^{-3}$·days)	Annual sum of daily maxima above 70 $\mu g \cdot m^{-3}$ (35 ppb)	Mid-high O_3 levels (Fleming et al. 2018), in line with WHO recommendations (WHO, 2021)	Annual summation	Fleming et al., (2018)
	P93.2 ($\mu g \cdot m^{-3}$)	Percentile 93.2 of the annual MDA8	High O_3 levels. Represents the 26th highest MDA8 value in a complete series (equiv. to 2008/50/EC Target Value exceedance if > 120 $\mu g \cdot m^{-3}$)*	Annual	EEA (2020)
Human health (peak O_3 levels)	4MDA8 ($\mu g \cdot m^{-3}$)	Fourth highest MDA8 in a year	Magnitude of photochemical episodes (i.e. peak short term exposure, equiv. to the 98th-99th percentile of the MDA8, Fleming et al. 2018; Colette et al., 2016)	Annual	Lefohn et al. (2018)
	IT90 (hours)	Annual sum of 1 h > 180 $\mu g \cdot m^{-3}$ (90 ppb)	Number of short extreme episodes. Used in 2008/50/EC (Information Threshold)	Annual summation	Querol et al. (2016)
Vegetation (mid-high O_3 levels)	AOT40veg ($\mu g \cdot m^{-3}$·hours)	Annual sum of 1 h > 80 $\mu g \cdot m^{-3}$ (40 ppb), during daylight in the growing season for crops & other vegetation in Europe	Risk assessment for agricultural crops and other vegetation. Used in 2008/50/EC	Annual summation (8:00–20:00 h CET in May-July)	Mills et al. (2018)
	AOT40 for ($\mu g \cdot m^{-3}$·hours)	Annual sum of 1 h > 80 $\mu g \cdot m^{-3}$ (40 ppb), during daylight in the growing season for forest trees in Europe	Risk assessment for forest trees (UNECE, 2010)	Annual summation (8:00–20:00 h CET in April-September)	EEA (2020)

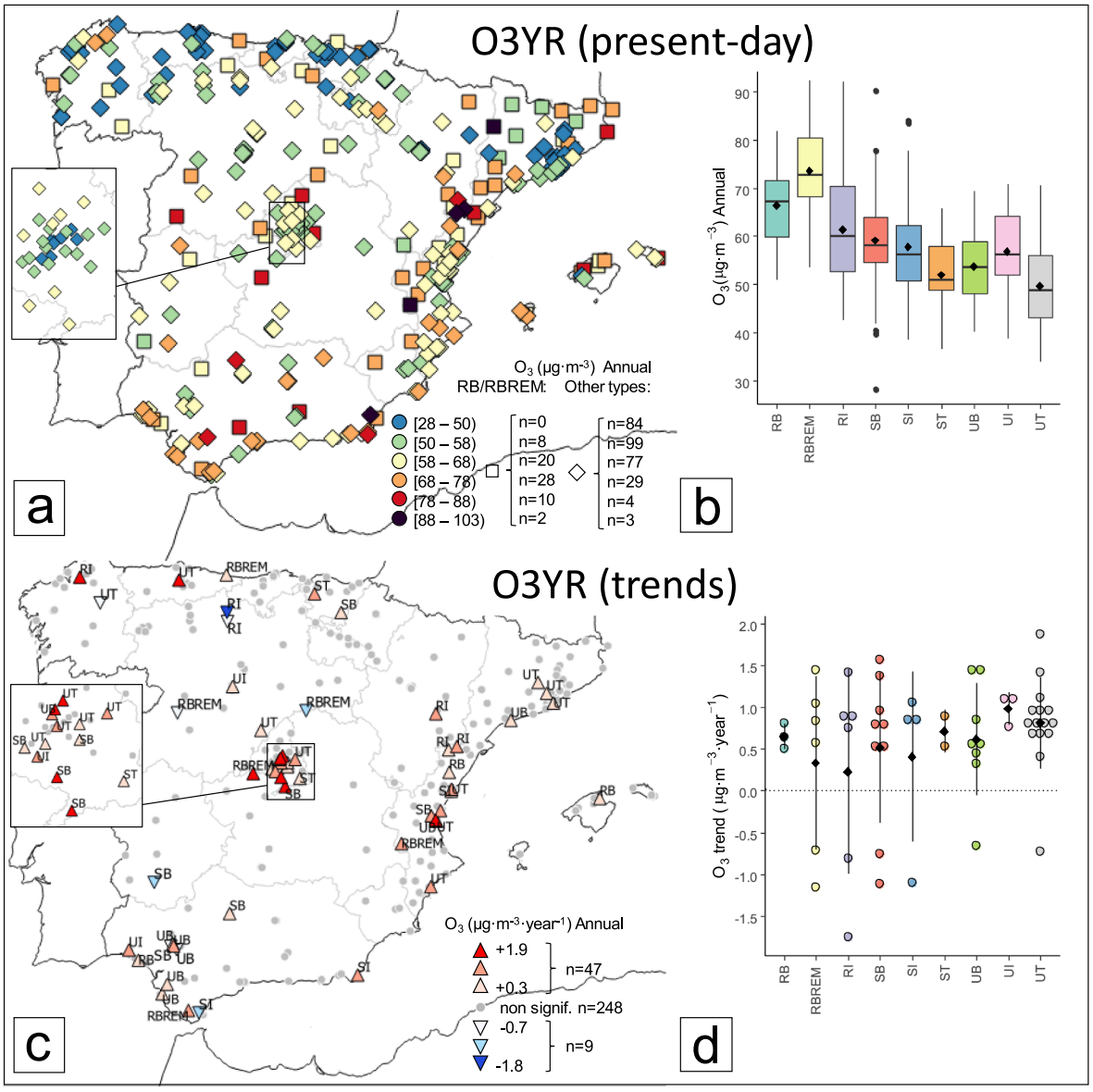

Fig. 2. (a, b) Present-day (2015–2019) annual O_3 (O3YR) concentrations from the 364 air quality stations (AQMSs) with valid data. (a) Spatial variation. Squares—rural background/regional (RB/RBREM) stations; circles—rest of the AQMSs. (b) Box-plot by station type. Upper numbers—number of stations of each type. (c, d) Statistically significant ($p < 0.05$) trends (2008–2019) from the 304 stations with valid data. (c) Spatial variation of the trends. (d) Annual variation by station type. Circles—trends from individual stations; black squares—averages; black lines—standard deviations. Upper numbers (top to bottom)—number of stations; trends; percentage of stations recording upward/downward trends. Abbreviations for stations are: UT/UI/UB—urban (traffic/industrial/background); ST/SI/SB—suburban (traffic/industrial/background); and RB/RI/RBREM—rural (background/industrial/regional background).

the Valencian Community and Cataluña (rural industrial AQMSs). We believe that these last three industrial AQMSs, which, based on several metrics (see below), recorded among the highest O_3 levels, should have their classifications change because the associated thermal power plant (Andorra, E-PRTR Code 3530) has permanently stopped operating in 2020. The peak O3YR levels (up to 103 $\mu g \cdot m^{-3}$) were recorded at high-elevation rural AQMSs, where nocturnal consumption of O_3 (if occurring) is much less pronounced as they are normally located far from fresh emission sources of O_3-consuming compounds, and also, if located above the planetary boundary layer, may have a continuous supply of O_3 from reservoir layers (e.g., Millán et al., 2000, 2002; Chevalier et al., 2007).

The metrics used for the protection of human health focusing on the mid to high part of the O_3 distribution (SOMO35 and P93.2), are shown in Fig. 3. The SOMO35 also exhibited a clear Cantabrian–Mediterranean gradient (Fig. 3a, b). The lowest present-day SOMO35 values (<3,000 $\mu g \cdot m^{-3} \cdot$day) were recorded at 17% of the stations, mainly in the north and north-western regions and basically in urban and suburban environments (predominantly industrial, traffic, and some background sites) and in only a few AQMSs in the city centers of Sevilla, Algeciras–Gibraltar, Valencia, and Barcelona (but not in Madrid). Although no legal threshold has been set for SOMO35, we used a critical level of 6,000 $\mu g \cdot m^{-3} \cdot$day for this assessment, in line with the WHO recommendations (Ellingsen et al., 2008). In Spain, 45% of the AQMSs recorded O_3 concentrations above this critical level, mostly located in the central, southern, and Mediterranean regions (particularly in the Valencian Community and the southern Mediterranean), which accords with EEA (2020). Of particular relevance is that a large amount of the population is being exposed to SOMO35 levels that are damaging to human health as ~ 40% of the urban and suburban AQMSs (representing the most populated areas) recorded O_3 levels above the critical SOMO35 and were mostly found in/around Madrid. The highest SOMO35 levels

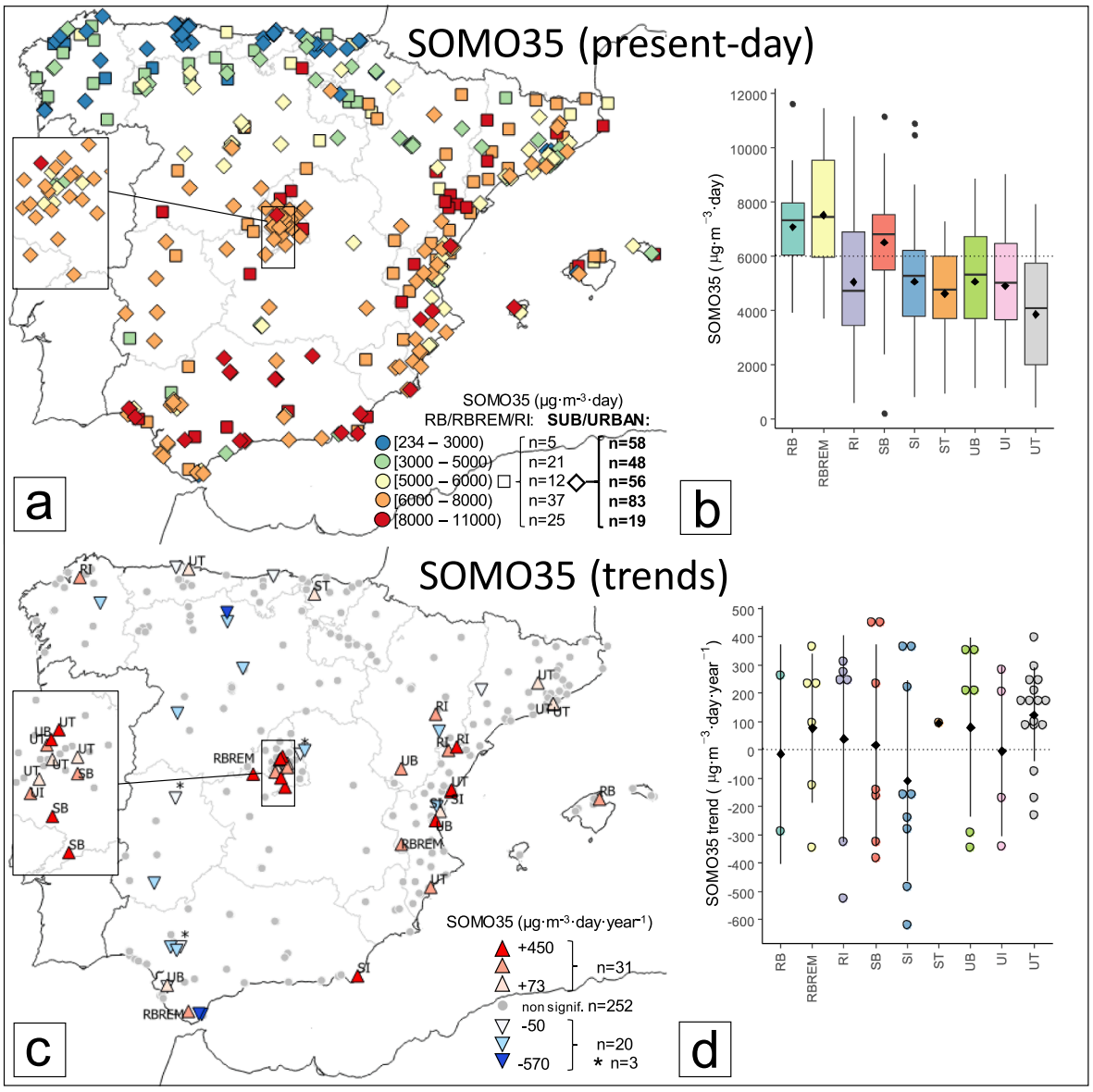

Fig. 3. (a, b) Present-day SOMO35 concentrations (μg·m^{-3}·day) for 2015–2019 from the 364 stations with valid data. (a) Spatial variation. (b) Box-plot by station type. Upper numbers—number of stations of each type. (c, d) Statistically significant ($p < 0.05$) trends in SOMO35 (2008–2019) (μg·m^{-3}·day·year^{-1}) from the 303 stations with valid data. (c) Spatial variation of the trends. (d) Annual variation by station type. Circles—trends from individual stations; black squares—averages; black lines—standard deviations. Upper numbers (top to bottom)—number of stations; trends; percentage of stations recording upward/downward trends. (e–h) Same captions as for (a–d), respectively, but for the percentile 93.2 of the daily maximum 8-hour average (MDA8), P93.2. (b, f) Horizontal lines in SOMO35 and P93.2 —critical level of 6,000 μg·m^{-3}·day (Ellingsen et al., 2008); the Directive's Target Value (120 μg·m^{-3}). Abbreviations for stations are: UT/UI/UB—urban (traffic/industrial/background); ST/SI/SB—suburban (traffic/industrial/background); and RB/RI/RBREM—rural (background/industrial/regional background).

(8,000–11,600 μg·m^{-3}·day) were recorded at 62% of the rural AQMSs and 5% at non-rural (i.e., urban and suburban). The only non-rural AQMSs that recorded such high SOMO35 levels were mostly in Andalucía and the southern Mediterranean regions.

The assessment of the metric P93.2 is shown in Fig. 3e, f. The Europe's TV was exceeded at > 20% of the Spanish AQMSs, and consistently with EEA (2020), mostly located in/around Madrid, Extremadura, Andalucía, northern Barcelona and a few sites in the Valencian Community. The P93.2 hotspots (>130 μg·m^{-3}) were mainly detected at rural background/regional stations downwind of large urban plumes (e.g., Millán et al., 1997, 2000, 2002; Gangoiti et al., 2001; Saiz-Lopez et al., 2009; Dieguez et al., 2009, 2014; Querol et al., 2017, 2018), such as in/around Madrid, northern Barcelona, interior Valencian Community, in some rural/suburban background AQMSs in the Guadalquivir Valley or Andalucía. Of relevance is that the only non-rural or regional sites with extreme P93.2 levels were only located in the interior of the Guadalquivir Valley and in/around Madrid. As with other metrics, low P93.2 concentrations were recorded in AQMSs located in the north and north-west, mostly in high-traffic and industrial environments. As expected, the lowest P93.2 values were recorded in the urban traffic AQMSs (Fig. 3f) because these AQMSs tend to be highly affected by NO titration and the ozonolysis of VOCs from traffic emissions. However, we detected high P93.2 values (up to 134 μg·m^{-3}) at eight urban traffic AQMSs, all influenced by the Madrid pollution plume.

The metrics used to assess human exposure to peak O_3 levels (4MDA8 and IT90) are shown in Fig. 4. More than 16% of the AQMSs recorded at least one annual IT90 exceedance in 2015–2019 (Fig. 4e,f). The IT90 hotspots were only located downwind of large precursor emitters, such

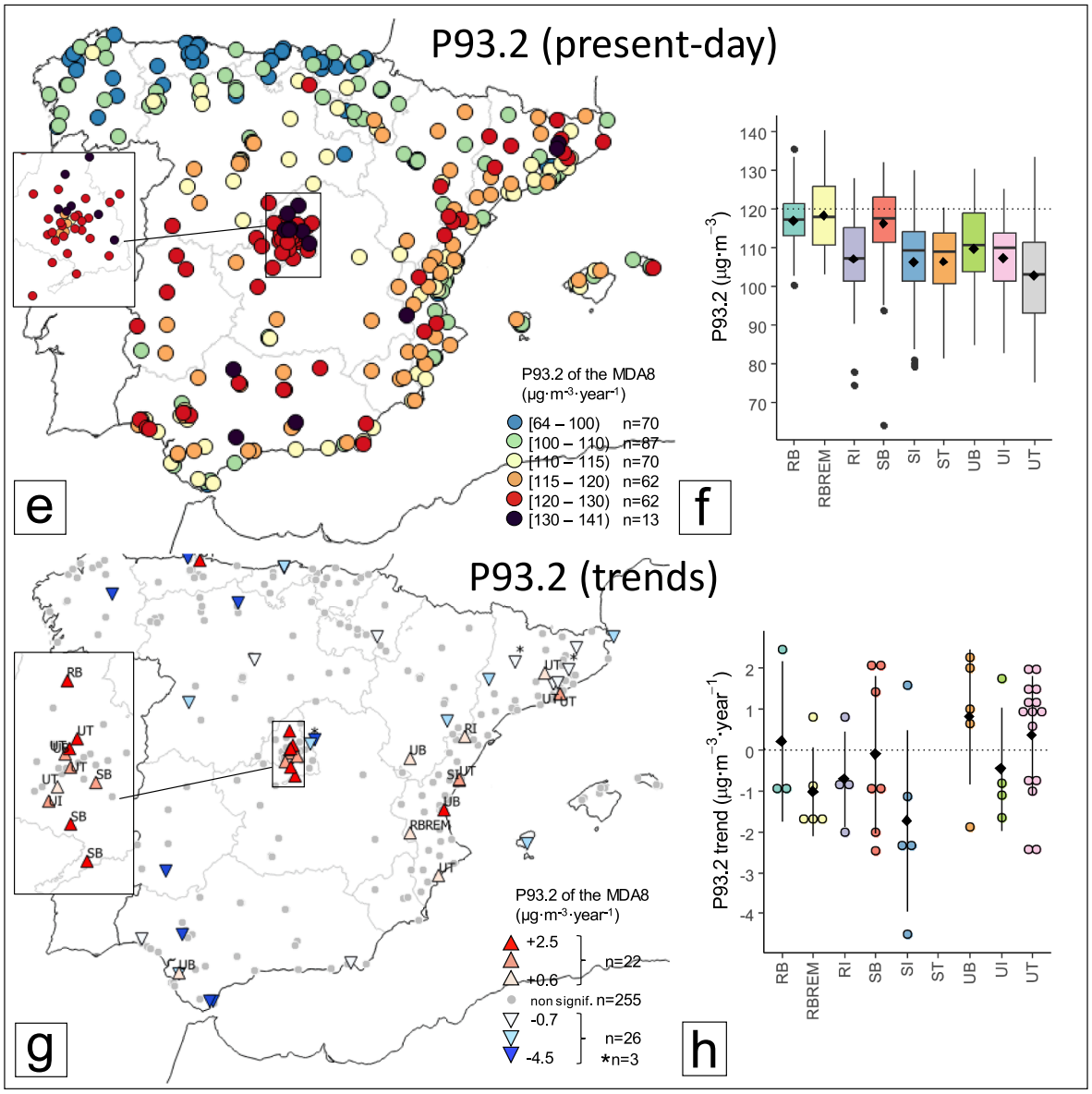

Fig. 3. (*continued*).

as northern Barcelona (rural/suburban background—18 exceed·year^{-1}), Madrid (regional and suburban background—10 exceed·year^{-1}) and, unlike the other metrics, the industrial area of Puertollano (rural industrial—9 exceed·year^{-1}). To a lesser extent, urban background AQMS in Extremadura and Sevilla, and an EMEP AQMS on the Atlantic coast of Galicia also exceeded the IT90 a few times a year (3–4 exceed·year^{-1}). This spatial pattern is similar to that for 2000–2015, as presented in Querol et al. (2016) but with certain differences in the northern regions.

The 4MDA8 and IT90 assessments indicate that several AQMSs (in some cases, even of traffic type, with potentially high NO concentrations) usually recorded very high O_3 concentrations due to contributions from pollution plumes transported from distant (tens of kilometers) urban and industrial areas due to the end-of-the-tail-of-the-plume (Millán et al., 2000). In these cases, the current type of AQMS is irrelevant because the contribution of regional O_3 from such plumes is the cause of the high-O_3 episodes. This indicates that the classification of stations used for O_3 assessment should be modified (Millán et al., 2000; Escudero et al., 2014; Tapia et al., 2016; Querol et al., 2016, 2017, 2018).

The metrics used here to assess the protection of vegetation and forests are shown in Figure S1.4. For the protection of vegetation (AOT40veg), the Directive has set a target value of 18,000 µg·m^{-3}·h, averaged over 5 years, together with a critical level for agricultural crops of 6,000 µg·m^{-3}·h as a long-term objective, with value by 2020. For the protection of forests (AOT40for), a critical level of 10,000 µg·m^{-3}·h has been recommended by UNECE (2010). We used the 133 available rural background/regional and suburban background AQMSs to assess the exposure of crops and natural ecosystems to O_3 (EC, 2008). The spatial variation of the AOT40, shown in Figure S1.4 also follows the Cantabrian–Mediterranean gradient and accords well with Mills et al. (2018) and EEA (2020).

Europe's AOT40veg target value was exceeded at > 50% of the rural and suburban background AQMSs across the country, except for in the north and north-west regions, and the LTO was exceeded at 93% of the AQMSs, except for at a few north-western sites. The highest AOT40veg values (24,000—34,000 µg·m^{-3}·h) were mostly found in Cataluña, southern Valencian Community, and Madrid, with the peak values occurring especially in Andalucía. The critical level for the AOT40 for (10,000 µg·m^{-3}·h) was systematically exceeded (at 95% of the AQMSs),

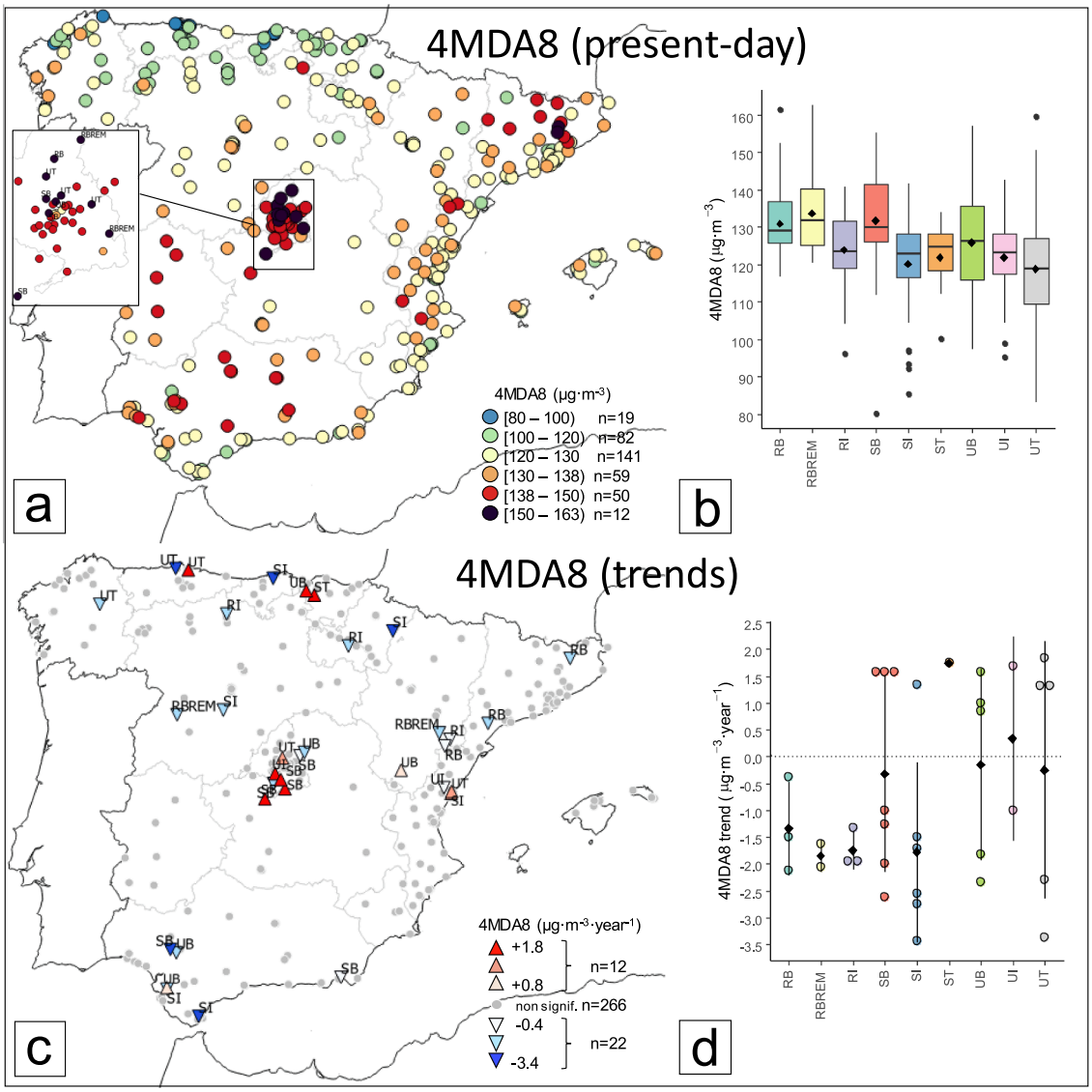

Fig. 4. (a, b) Present-day fourth daily maximum 8-hour average (4MDA8) concentrations ($\mu g \cdot m^{-3}$) for 2015–2019 from the 363 stations with valid data. (a) Spatial variation. (b) Box-plot by station type. Upper numbers—number of stations of each type. (c, d) Statistically significant ($p < 0.05$) trends in 4MDA8 (2008–2019) ($\mu g \cdot m^{-3} \cdot year^{-1}$) from the 300 stations with valid data. (c) Spatial variation of the trends. (d) Annual variation by station type. Circles—trends from individual stations; black squares—averages; black lines—standard deviations. Upper numbers (top to bottom)—number of stations; trends; percentage of stations recording upward/downward trends. (e–g) Same caption as for (a–c), but for IT90, 364 instead of 363 for the present-day and 304 sites instead of 300 for the trends. The units for IT90 are 'hours' (of exceedance of Europe's Information Threshold, 180 $\mu g \cdot m^{-3}$). Abbreviations for stations are: UT/UI/UB—urban (traffic/industrial/background); ST/SI/SB—suburban (traffic/industrial/background); and RB/RI/RBREM—rural (background/industrial/regional background).

also with the exception of a few north-western sites, and the highest levels (up to 56,000 $\mu g \cdot m^{-3} \cdot h$) followed a similar spatial pattern as for the AOT40veg. The occurrence of high AOT40 levels is relevant in Spain due to the high biodiversity in the Iberian Peninsula and the large number of natural protected areas that are potentially being affected (Escudero et al., 2016). It should be noted that concentration-based metrics such as AOT40, are not the most suitable indicators of actual damage to vegetation, as they should ideally be based on flux (or stomatal uptake) of O_3 (Mills et al., 2018 and references therein), especially under Mediterranean conditions with frequent drought periods coinciding with the highest O_3 levels.

3.2. Classification of O_3 atmospheric regions (R1–R4)

Results show a present-day O_3 spatial variation that is a function of the part of the O_3 distribution being considered. As the O_3 metrics focus on higher parts of the O_3 distribution, the clear climatic Cantabrian–Mediterranean gradient observed when considering lower O_3 metrics, tends to attenuate by highlighting O_3 hotspot regions that have relevant local/regional O_3 formation. These findings are further supported in Section S4 (supplemental) which examines the correlations between meteorological parameters that are relevant to O_3, geographical location, and O_3 levels.

From our results and background information on the phenomenology of high-O_3 episodes from previous studies (e.g., Millán et al., 1997, 2000; Dieguez et al., 2009; Dieguez et al., 2014; Gangoiti et al., 2001; Millán, 2014; ; Querol et al., 2016, 2017, 2018; Escudero et al., 2019), we present a conceptual model in Fig. 5 that classifies Spanish areas in atmospheric regions (R1 to R4) according to their O_3 pollution patterns. The bottom bar plot depicts the contributions of O_3 in each of the atmospheric regions under typical O_3 season conditions and also during episodic events.

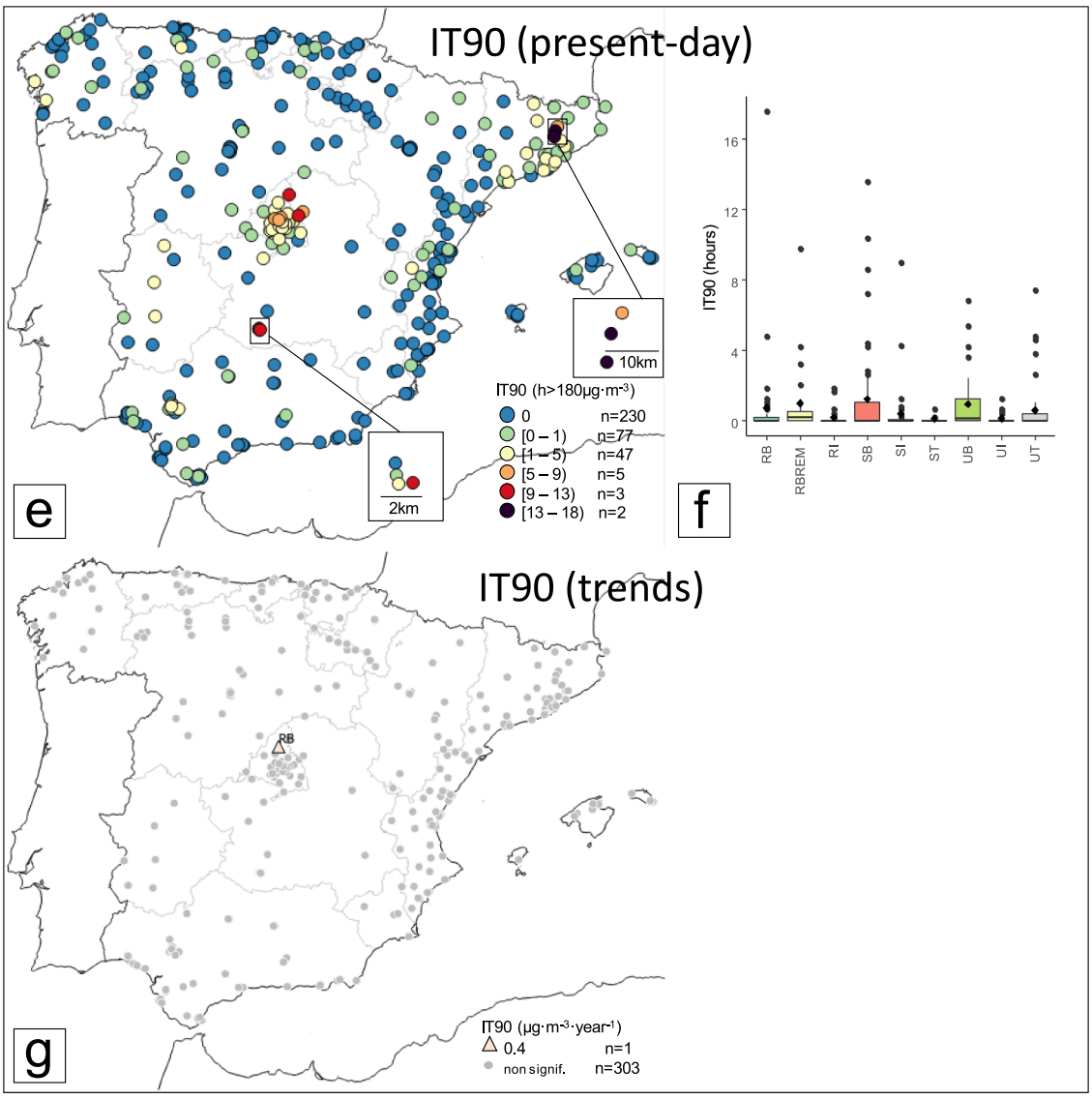

Fig. 4. (*continued*).

The northern and north-western areas, which had the lowest concentrations for all the O_3 metrics, mainly due to meteorological conditions that do not favor O_3 production (Fig. S1.1c–f and Fig. S4.1) (Gangoiti et al., 2002, 2006; Saavedra et al., 2012), are referred to as Type 1 regions (R1). Conversely, in the central, southern, and Mediterranean areas, the O_3 levels tended to be higher due to large precursor anthropogenic and biogenic emissions, the prevailing meteorological conditions in the warm seasons, and the characteristic orography that favors the production and accumulation of O_3 (Millán et al., 1997, 2000; Gangoiti et al., 2001).

High-O_3 episodes are generated by large emissions of precursors from the metropolitan areas of Madrid, Barcelona, Sevilla, and Valencia, and the industrial areas of Puertollano, Huelva, Tarragona and Castellón (Millán et al., 1997, 2000, 2002; Gangoiti et al., 2001; Saiz-Lopez et al., 2009; Dieguez et al., 2009, 2014; Querol et al., 2017, 2018; Massagué et al., 2019, 2021; in 't Veld et al., 2021). There, even if the regional (Europe-scale) hemispheric and stratospheric O_3 contributions might be high in spring–summer, the local/regional production accounts for the occurrence of very acute O_3 episodes downwind of these areas (Pay et al., 2019). We refer to these regions as Type 3 (R3). This type might also include the area impacted downwind of the core and commuting zones of the Portuguese cities of Porto and Lisbon (e.g., Dieguez et al., 2009; Monteiro et al., 2012; Cerrato-Alvarez et al., 2020).

Although, in most metrics, the industrial area of Puertollano did not record particularly high O_3 concentrations, it did have among the highest national IT90 levels (5–9 IT annual exceedances), although only at two closely located AQMSs. Other nearby AQMSs (within 5 km) did not exceed Europe's IT, pointing to the direct impact of precursor emissions from a localized industrial estate accumulating in a closed basin (e.g., Dieguez et al., 2009; Millán, 2009). Accordingly, we qualify this region as Type 4 (R4) —a peculiar R3 associated with very local effects.

The O_3 generated in R3-type regions affects other regions, such as Extremadura, Aragón, Navarra, La Rioja, northern Castilla–La Mancha, the Balearic Islands, southern País Vasco, and southern Castilla y León. These regions have intermediate O_3 concentrations between R1 and R3, but are still impacted by high stable background levels; these are the Type 2 regions (R2).

This type of analysis is crucial for the establishment of an effective national Ozone Mitigation Plan, since concisely identifies the areas to be prioritized for policy implementation according to the severity of O_3 pollution. After identifying the areas where emission reduction policies require prioritization, the distinctive characteristics of each area will demand the implementation of specific measures at the local/regional

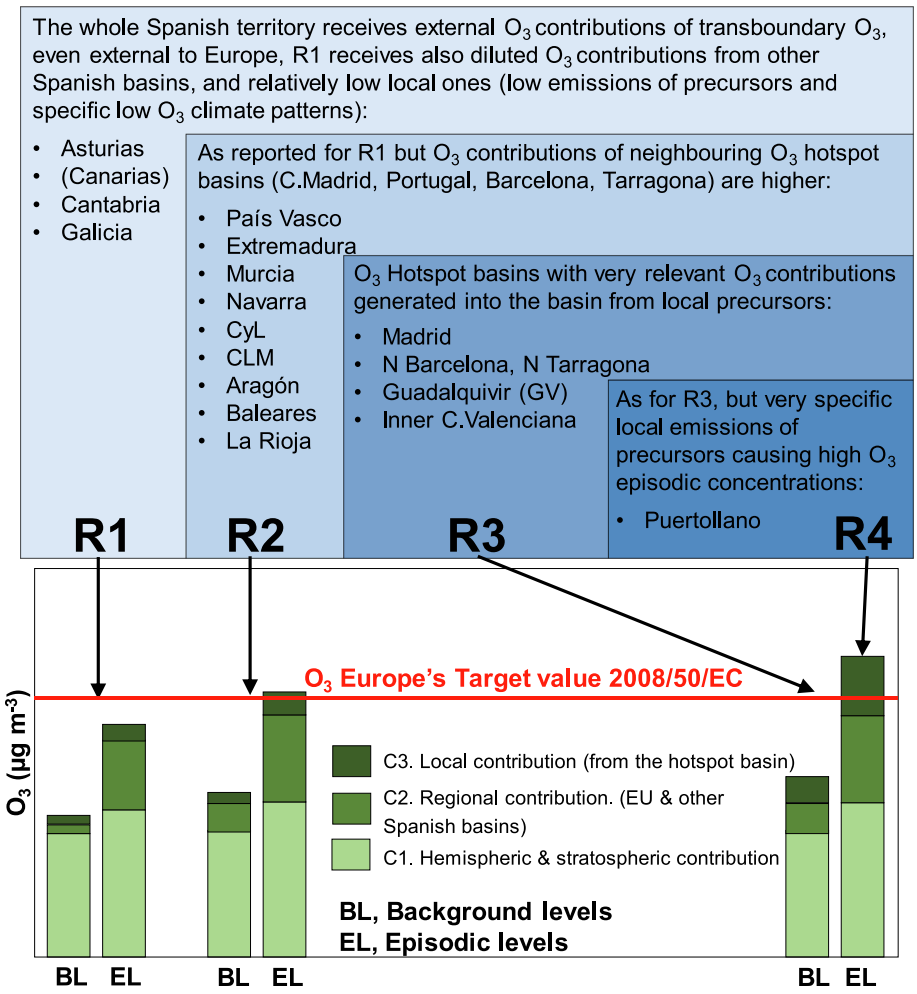

Fig. 5. Conceptual model of the classification of O_3 regions (R1–R4) in Spain based on the intensity and frequency of high-O_3 episodes and the origin of the O_3 and its precursors. CyL—Castilla y León; CLM—Castilla–La Mancha. Note that the bottom bars do not reflect actual O_3 concentrations, as the O_3 contributions are indicative and based on previous literature and the results obtained in this study.

level.

3.3. Trends (2008–2019)

The detected trends are discussed below, the figures we refer to can be found in Section 3.1, and the individual time series of the (statistically significant) trends can be consulted for each metric and AQMSs in Section S5 (supplemental).

Most AQMSs (82%) recorded no trends in annual mean O_3 concentrations (O3YR) (Fig. 2c, d). Trends in this mid-level metric show a spatial variation dominated by upward trends, with 84% of the trends being upward, mostly recorded at suburban and urban AQMSs, especially in Madrid, along with the highest national increases (+1.9 µg·m^{-3}·year^{-1}), in the Valencian Community, and, to a lesser extent, in some other dispersed AQMSs. The most consistent increases (highest number of upward trends, highest upward mean averages, and lowest standard deviations) were found at urban stations, especially those in high-traffic locations (Fig. 2d). These upward urban trends are consistent with several studies on Europe, Spain, and neighboring countries from the 2000 s (e.g., Sicard et al., 2013, 2016, 2020; Paoletti et al., 2014; Colette et al., 2016; Querol et al., 2016), and have been attributed to a lower titration of O_3 by NO due to the establishment of vehicle emissions regulations in the EU or to the effect of decreasing NOx in VOC-limited O_3 regimes (Colette et al., 2011; Lefohn et al., 2018; Sicard et al., 2020, 2021). The few downward O3YR trends were recorded mainly at dispersed industrial AQMSs located in northern regions or in western Andalucía (up to −1.8 µg·m^{-3}·year^{-1}), including Sevilla.

Considering the trends from the rural background/regional AQMSs (representative of baseline O_3 levels, Colette et al., 2016), the two EMEP AQMSs (located in western coastal Galicia and in the Balearic Islands), which better represent the regional O_3 behavior in Spain (Dieguez et al., 2009), did not record any trends over the studied period. However, we found two continental EMEP AQMSs that recorded downward trends, and several rural background/regional AQMSs that recorded upward trends (Fig. 2c). These rural background/regional AQMSs that recorded the trends probably do not represent baseline O_3 because they may be affected by O_3 from R3 areas and/or transport of air masses from highly polluted urban/industrial areas (e.g., Millán et al., 2000; Dieguez et al., 2009, 2014; Escudero et al., 2014, 2016; Querol et al., 2016, 2017, 2018).

Several studies have reported O3YR decreases at most rural background/regional AQMSs in Europe (Paoletti et al., 2014; Colette et al., 2016; Sicard et al., 2016; Lefohn et al., 2018), attributing them to the reduction in NOx and VOC emissions due to the application of stringent vehicle emissions standards, improvements in the management of solvents, and the use of stack gas-reduction technologies from the 2000 s (Monks et al., 2015; EEA, 2019; Sicard, 2021). However, mixed behaviors were reported for Spain, such as: (i) Wilson et al. (2012), who determined downward O_3 trends for 1996–2005 in a period when NOx emissions slightly increased and VOCs showed almost no variation in Spain, as opposed to the general increasing O_3 trends with decreasing NOx and VOCS emissions in Europe; (ii) Querol et al. (2016) found no

trends in rural background AQMSs for 2000–2015, in a period with little decline in NO_2 from 2000; (iii) Sicard et al. (2013) quantified a slight O_3 increase in 2000–2010 on the Spanish coast, attributing it to a significant increase in NOx emissions in 1990–2010; and (iv) Sicard et al. (2020) found a slight O_3 decrease in 2005–2014 during a period of high NOx decreases and less-intense VOC decreases. Thus, the time period (and length) selected for trend assessment is important because it might give different results to other studies (Fleming et al., 2018) due to inter-annual variability (especially for short periods) and the different extents to which the drivers of O_3 variability may have varied during a certain period (e.g., Lefohn et al., 2017).

The assessment of trends for the SOMO35 and P93.2 metrics (Fig. 3c, d, g, h) also indicates that most AQMSs did not follow trends (at 83% and 84% of the AQMSs, respectively). Among the detected trends, however, upward trends dominated for SOMO35 (at 61% of the AQMSs), while, conversely, for P93.2, downward trends dominated (54%). Although the SOMO35 and P93.2 trends had heterogeneous patterns with respect to station type (Fig. 3d, h), 74% and 90% of the upward trends, respectively, were recorded at urban and suburban AQMSs, indicating that the most populated areas were being exposed to increasing SOMO35 and P93.2 levels, while the other station types showed no dominant trends.

The results show that the AQMSs in Madrid again recorded the highest proportion of upward trends for these metrics, with 35% and 45% of them being recorded in this area for SOMO35 and P93.2, respectively. Most of the P93.2 upward trends in/around Madrid (90%) were detected at urban and suburban sites (i.e., in highly populated areas). Moreover, most of these AQMSs exceeded the equivalent of Europe's TV, with high values of up to 134 $\mu g \cdot m^{-3}$, thus evidencing a relevant high risk and increasing O_3 exposure to the population in this area. After Madrid, the Valencian Community was the second R3 region that recorded a higher proportion of upward trends for the SOMO35 and P93.2 (26% and 27%, respectively, at the national level) (Fig. 3). Also, the highest increasing intensities were detected in Madrid (SOMO35 at + 454 $\mu g \cdot m^{-3} \cdot day \cdot year^{-1}$, P93.2 at + 2.4 $\mu g \cdot m^{-3} \cdot year^{-1}$).

Conversely, the city of Sevilla was the only large Spanish city that recorded downward trends for both metrics. It also had among the largest decreasing national P93.2 slope (up to −2.5 $\mu g \cdot m^{-3} \cdot year^{-1}$). Other AQMSs that recorded downward SOMO35 (up to −566 $\mu g \cdot m^{-3} \cdot day \cdot year^{-1}$) and P93.2 (up to −4.5 $\mu g \cdot m^{-3} \cdot year^{-1}$) trends were in Gibraltar–Algeciras and Castilla y León, and in other dispersed locations, mainly in industrial environments. The spatial variation of the 2008–2019 SOMO35 trends is consistent with EEA (2020) in Spain for a very similar period (2009–2018), and different from Fleming et al. (2018) for a previous period (2000–2014), which found significantly fewer upward trends and a different spread.

The trends in the metrics focusing on peak O_3 concentrations were rare or practically non-existent (Fig. 4). For the 4MDA8 and IT90 metrics, the majority (89%) of the AQMSs, and all the AQMSs but one, respectively, recorded no trends. For 4MDA8, most of the trends (65%) were downward. Conversely, the only IT90 trend was upward, from a rural background AQMS located downwind (north-east) of the urban plume of Madrid. Interestingly, by using a less restrictive p-value ($p < 0.1$ instead of the $p < 0.05$; not shown), the other only trend detected in the whole country was upward, and recorded in a regional AQMS closely located to the other site in Madrid.

For 4MDA8 (Fig. 4c), no rural background/regional AQMSs recorded upward trends, and only five recorded downward trends (two of them EMEP sites), all located in the northern half of the country, and in line with Colette et al. (2016) for 2002–2012. Considering the other types of AQMSs, most of the upward 4MDA8 trends and the most-intense ones (up to + 1.8 $\mu g \cdot m^{-3} \cdot year^{-1}$) were again found in the Madrid area, in urban and suburban AQMSs, all in locations with high present-day 4MDA8 levels (Fig. 4a), along with some dispersed urban and suburban AQMSs in the Valencian Community and northern Spain. As for the other metrics, Sevilla was the only large Spanish city that recorded downward trends (up to −2.6 $\mu g \cdot m^{-3} \cdot year^{-1}$). General decreases in O_3 peaks have been reported in Europe since the 2000s (Sicard et al., 2013, 2016; Paoletti et al., 2014; Lefohn et al., 2017, 2018; Fleming et al., 2018), mainly being attributed to the reduction in NOx emissions resulting from vehicle emissions standards, but with slight decreases in Spain. Also, Fleming et al. (2018) found mostly downward trends in Europe in 2000–2014 in peak O_3 values (4MDA8 and other metrics), with the exception of two non-urban upward 4MDA8 trends in north-eastern Spain. Because peak O_3 concentrations mainly result from local *fresh* photochemistry, the decrease in peak O_3 and its related metrics in the most polluted European sites has been attributed to the decrease in European emissions of precursors (Colette et al., 2016).

As with the other metrics, for AOT40 metrics most AQMSs did not record any trends (at 88% and 84% of the AQMSs for AOT40veg and AOT40for, respectively; Figure S1.4). The results show a similar proportion of upward and downward trends for these metrics, and also spatial consistency with EEA (2020) for 2009–2018. The Madrid area again had the highest number of upward trends, and the most-intense increases (up to + 1,600 $\mu g \cdot m^{-3} \cdot h \cdot year^{-1}$ and up to + 3,000 $\mu g \cdot m^{-3} \cdot h \cdot year^{-1}$, respectively). Outside this area, we found very few upward trends in eastern Spain (high-elevation EMEP AQMSs in the Valencian Community and Andalucía). A few downward trends were found mostly in the south-west (around Sevilla, with the most intense decreases of up to −1,400 $\mu g \cdot m^{-3} \cdot h \cdot year^{-1}$ and up to −2,600 $\mu g \cdot m^{-3} \cdot h \cdot year^{-1}$ for AOTveg and AOTfor, respectively).

The results for the trend assessments show that a relatively low number of trends were detected in several areas, mostly in R3 types (i.e. O_3 hotspots). However, most of the AQMSs in our study did not record trends, regardless of the O_3 metrics considered, as has been found in other studies carried out on Europe or at the global level, analyzing similar lengths of time (e.g., Fleming et al., 2018; Mills et al., 2018; EEA, 2020). This is partly due to the meteorological sensitivity of O_3, which causes it to vary from year to year, therefore making the detection of trends challenging on such relatively short time-scales (Colette et al., 2016; Fleming et al., 2018).

Also, as described in Lefohn et al. (2017, 2018) and Yan et al. (2019), our results indicate that a common change in the distribution of O_3 concentrations can result in dissimilar trends for different metrics because they may differentially emphasize low, moderate, or high O_3 levels. Actually, it is not uncommon for one metric to show a negative trend while another shows a positive trend for the same O_3 time-series. We found that, as the assessed O_3 metrics along the O_3 distribution focused on higher O_3 concentrations (from O3YR to 4MDA8 and IT90), the number of detected trends decreased (Colette et al., 2016) and/or the proportion of downward versus upward trends increased (Table S1.2), sometimes even at the same AQMS (as also found by, e.g., Sicard et al., 2016; Lefohn et al., 2018). This latter pattern suggests a narrowing of the range of O_3 concentrations (e.g., Sicard et al., 2013; Paoletti et al., 2014; Simon et al., 2015). Lefohn et al. (2017, and references therein) indicated three main drivers that might contribute to this behavior, including changes in: (i) local/regional anthropogenic precursor emissions; (ii) O_3 contributions from long-range transport; and (iii) trends in meteorology and climate-driven biogenic emissions.

To account for the contrasting trends observed across the different O_3 hotspots (R3 regions) as revealed by our findings, it is crucial to comprehend their underlying causes and develop specific strategies aimed at reducing O_3 concentrations in each area, all of which should be taken into account in the Ozone Mitigation Plan.

4. Conclusions

To contribute to the development of Spain's Ozone Mitigation Plan, this work assesses the spatial variation and trends of seven tropospheric ozone (O_3) metrics relevant for human/ecosystems exposure and regulatory purposes, using data from 364 air quality monitoring stations (AQMSs).

Results show a present-day (2015–2019) spatial variation of O_3 that

is a function of the part of the O_3 distribution being considered. The metrics associated with moderate to high O_3 concentrations, show a clear increasing gradient due to climate characteristics between the northern (Cantabrian) and the Mediterranean coasts. As metrics focus towards the upper end of the O_3 distribution, this gradient is attenuated in favor of hotspots, pointing to relevant local/regional O_3 formation.

The mid-high sector of the O_3 distribution was assessed with metrics for health protection (SOMO35 and P93.2) and vegetation protection (AOT40 for crops and forests). The proportion of AQMSs exceeding the thresholds of these metrics were remarkable, highlighting the health and environmental impact of O_3 in Spain. The areas with the highest SOMO35 and P93.2 levels were Madrid, the Mediterranean regions and, to a lesser extent, Extremadura and Andalucía. Europe's target value exceedances (analyzed here with P93.2 values) were mostly recorded downwind of large urban plumes, at regional background sites, but also at urban sites in the Guadalquivir Valley (Andalucía) and Madrid. The highest values of O_3 metrics associated with peak concentrations (4MDA8 and IT90) were recorded in Madrid (including urban sites), northern Barcelona and, due to local industrial contributions, at Puertollano.

Based on our findings and previous literature, we propose a classification of atmospheric regions in Spain into four types (R1–R4) derived from their O_3 pollution patterns. R1 covers the northern and northwestern areas, which receive mostly external O_3 contributions. R2 includes north-eastern and continental areas with the same contributions as for R1, but larger contributions from neighboring O_3 hotspots. R3 comprises the O_3 hotspots, i.e., Madrid, northern Barcelona, the Guadalquivir Valley, and inland Valencian Community. Finally, R4 covers a specific area near Puertollano, with large local industrial emissions that cause acute high-O_3 episodes.

Results from the trends assessment (2008–2019) point to a compression of the range of O_3 concentrations. Most of the AQMSs did not record statistically significant trends; however, trends were detected in many areas, mostly in R3 regions. These regions followed contrasting O_3 trends, where (i) the Madrid area recorded most of the upward trends for all the metrics (often with the highest increasing rates), implying increasing ozone levels associated with both chronic and episodic exposure, (ii) the Valencian Community area had a mixed variation pattern, (iii) the areas downwind of Barcelona, the Puertollano closed basin and the Guadalquivir Valley followed no O_3 trends, and (iv) Sevilla was the only large Spanish urban area that recorded generalized decreasing trends.

The evaluation of the national O_3-monitoring network also show that (i) the current classification of AQMSs is devised for primary pollutants and may not be appropriate for O_3 assessment because, for example, urban traffic AQMSs downwind of urban pollution plumes recorded extreme O_3 concentrations, (ii) several regional background AQMSs (some of them EMEP) that recorded trends are not necessarily representing the baseline O_3, as some trends were driven by polluted air masses being regionally transported and, (iii) the classification of some AQMSs should be updated as the nearby emissions sources originally considered to define them, have changed or disappeared.

In the near future, the formulation of national plans for the mitigation of O_3 will be required. Consequently, this study has implications that extend beyond its obvious local scope, as it highlights the importance of an "atmospheric region" approach. Such an approach enables the identification of areas to be prioritized for policy implementation according to the severity of O_3 pollution, as opposed to the commonly adopted national-level approach seen in other works. Additionally, the results indicate that O_3 may exhibit contrasting trends across atmospheric regions within a given country. This emphasizes the significance of designing effective mitigation measures that may vary at a local/regional scale and allow assessing the effectiveness of already implemented interventions. This work also represents a step towards a better understanding of the relation between O_3 metrics for the protection of human health and vegetation, and changes in the distribution of O_3 concentrations in Spain. Modeling studies should be conducted to identify cost-effective policy measures to abate O_3. The modeling framework must be able to reproduce local/regional O_3 formation using high-resolution modeling and emissions inventories, and account for regional, transboundary, hemispheric, and stratospheric O_3 contributions.

CRediT authorship contribution statement

Jordi Massagué: Conceptualization, Data curation, Formal analysis, Investigation, Methodology, Software, Validation, Visualization, Writing – original draft, Writing – review & editing. **Miguel Escudero:** Conceptualization, Formal analysis, Investigation, Methodology, Validation, Visualization, Writing – original draft, Writing – review & editing. **Andrés Alastuey:** Conceptualization, Formal analysis, Funding acquisition, Investigation, Methodology, Project administration, Resources, Supervision, Validation, Visualization, Writing – review & editing. **Enrique Mantilla:** Formal analysis, Investigation, Supervision, Validation, Writing – review & editing. **Eliseo Monfort:** Formal analysis, Investigation, Supervision, Validation, Writing – review & editing. **Gotzon Gangoiti:** Formal analysis, Investigation, Supervision, Validation, Writing – review & editing. **Carlos Pérez García-Pando:** Formal analysis, Investigation, Supervision, Validation, Writing – review & editing. **Xavier Querol:** Conceptualization, Formal analysis, Funding acquisition, Investigation, Methodology, Project administration, Resources, Supervision, Validation, Visualization, Writing – original draft, Writing – review & editing.

Declaration of Competing Interest

The authors declare that they have no known competing financial interests or personal relationships that could have appeared to influence the work reported in this paper.

Data availability

The data that support the findings of this study are openly available. Links have been provided in the article or its supplementary materials.

Acknowledgements

The present work was supported by the Spanish Ministry of Ecological Transition and Demographic Challenge (Spanish National Ozone Plan); European Union's Horizon 2020 research and innovation program under grant agreement; and the "Agencia Estatal de Investigación'' from the Spanish Ministry of Science and Innovation, and FEDER funds, under the projects CAIAC (PID2019-108990RB-I00) and HOUSE (CGL2016-78594-R). This work was also supported by the Autonomous Government of Valencia (GVA) through the Valencian Institute for Business Competitiveness (IVACE) by means of the project Gaia (IMAMCA/2022/1). Carlos Pérez García-Pando acknowledges the support of the AXA Research Fund. We would like to thank M.Mar Hervás (Inypsa CW Infrastructures SL) for providing air quality data.

Appendix A. Supplementary data

Supplementary data to this article can be found online at https://doi.org/10.1016/j.envint.2023.107961.

References

Batista e Silva, F., Dijkstra, L., Poelman, H., 2021. The JRC-GEOSTAT 2018 population grid. JRC Technical Report (forthcoming).

Carslaw, D., Ropkins, K., 2012. Openair – an R package for air quality data analysis. Environ. Model. Softw. 27–28, 52–61.

Castellanos, P., Boersma, K., 2012. Reductions in nitrogen oxides over Europe driven by environmental policy and economic recession. Sci Rep 2, 265. https://doi.org/10.1038/srep00265, 2012.

Cerrato-Alvarez, M., Núñez-Corchero, M., Miró-Rodríguez, C., et al., 2020. Synoptic circulation patterns and local sources associated to high concentrations of tropospheric ozone in rural and suburban areas in southwestern Spain. Air Qual Atmos Health 13, 97–108. https://doi.org/10.1007/s11869-019-00774-w.

Chevalier, A., Gheusi, F., Delmas, R., Ordonez, C., Sarrat, C., Zbinden, R., Thouret, V., Athier, G., Cousin, J.M., 2007. Influence of altitude on ozone levels and variability in the lower troposphere: a ground-based study for western Europe over the period 2001–2004. Atmos. Chem. Phys. 7, 4311–4326.

Coates, J., Mar, K.A., Ojha, N., Butler, T., 2016. M.: The influence of temperature on ozone production under varying NO_x conditions – a modelling study. Atmos. Chem. Phys. 16, 11601–11615. https://doi.org/10.5194/acp-16-11601-2016.

Colette, A., Aas, W., Banin, L., Braban, C.F., Ferm, M., et al., 2016. Air pollution trends in the EMEP region between 1990 and 2012. Joint Report of the EMEP Task Force on Measurements and Modelling (TFMM), Chemical Co-ordinating Centre (CCC), Meteorological Synthesizing Centre-East (MSC-E), Meteorological Synthesizing Centre-West (MSC-W). EMEP: TFMM/CCC/MSC-E/MSC-W Trend Report (01/2016).

Colette, A., Granier, C., Hodnebrog, Ø., Jakobs, H., Maurizi, A., Nyiri, A., Bessagnet, B., D'Angiola, A., D'Isidoro, M., Gauss, M., Meleux, F., Memmesheimer, M., Mieville, A., Rouïl, L., Russo, F., Solberg, S., Stordal, F., Tampieri, F., 2011. Air quality trends in Europe over the past decade: a first multi-model assessment. Atmos. Chem. Phys. 11, 11657–11678. https://doi.org/10.5194/acp-11-11657-2011.

Diéguez, J.J., Millán, M., Padilla, L., Palau, J.L., 2009. Estudio y evaluación de la contaminación atmosférica por ozono troposférico en España, CEAM Report for the Ministry of Agriculture, Food and Environment, INF FIN/O3/2009, 372 pp.

Diéguez, J.J., Calatayud, V., Mantilla, E., 2014. Informe Final, Memoria Técnica Proyecto CONOZE, CONtaminación por OZono en España, CEAM Report for the Ministry of Agriculture, Food and Environment, Fundación Biodiversidad, 137 pp.

EC, 2004, Directive 2004/107/EC of the European Parliament and of the Council of 15 December 2004 relating to arsenic, cadmium, mercury, nickel and polycyclic aromatic hydrocarbons in ambient air (OJ L 23, 26.1.2005, pp. 3-16), https://eur-lex.europa.eu/eli/dir/2004/107/oj, last access: 30 December 2022.

EC. Directive 2008/50/EC, Of The European Parliament And Of The Council of 21 May 2008 on ambient air quality and cleaner air for Europe http://eur-lex.europa.eu/legal-content/ES/TXT/?uri=CELEX:32008L0050, last access: 30 December 2022.

EC, 2011. Commission Implementing Decision No 2011/850/EU of 12 December 2011 laying down rules for Directives 2004/107/EC and 2008/50/EC of the European Parliament and of the Council as regards the reciprocal exchange of information and reporting on ambient air quality (OJ L 335, 17.12.2011, p. 86-106) https://eur-lex.europa.eu/legal-content/EN/TXT/?uri=CELEX%3A32011D0850, last access: 30 December 2022.

EEA: European Union Emission Inventory Report 1990-2017 under the UNECE Convention on Long-Range Transboundary Air Pollution (LRTAP). EEA Report No 08/2019, Copenhagen, p. 148pp, 1977-8449, 2019.

EEA: Air quality in Europe–2020 report, European Environment Agency. EEA Report, No 09/2020 (ISSN 1977-8449), 160 pp. doi: 10.2800/786656, 2020.

EEA: Status report of air quality in Europe for year 2020. Eionet Report – ETC/ATNI 2021/8, 2021.

Ellingsen, K., Gauss, M., Van Dingenen, R., Dentener, F.J., Emberson, L., Fiore, A.M., Schultz, M.G., Stevenson, D.S., et al., 2008. Global ozone and air quality: a multi-model assessment of risks to human health and crops. Atmos. Chem. Phys. Discuss. 8, 2163–2223.

Escudero, M., Lozano, A., Hierro, J., del Valle, J., Mantilla, E., 2014. Urban influence on increasing ozone concentrations in a characteristic Mediterranean agglomeration. Atmos. Environ. 99, pp. 322–332. 10.1016/j.atmosenv.2014.09.061.

Escudero, M., Lozano, A., Hierro, J., Tapia, O., del Valle, J., Alastuey, A., Moreno, T., Anzano, J., Querol, X., 2016. Assessment of the variability of atmospheric pollution in National Parks of mainland Spain. Atmos. Environ. 132, 332–344. https://doi.org/10.1016/j.atmosenv.2016.03.006.

Escudero, M., Segers, A., Kranenburg, R., Querol, X., Alastuey, A., Borge, R., de la Paz, D., Gangoiti, G., Schaap, M., 2019. Analysis of summer O3 in the Madrid air basin with the LOTOS-EUROS chemical transport model. Atmos. Chem. Phys. 19, 14211–14232. https://doi.org/10.5194/acp-19-14211-2019.

Fleming, Z.L., Doherty, R.M., von Schneidemesser, E., Malley, C.S., Cooper, O.R., Pinto, J.P., Colette, A., Xu, X., Simpson, D., Schultz, M.G., Lefohn, A.S., Hamad, S., Moolla, R., Solberg, S., Feng, Z., 2018. Tropospheric Ozone Assessment Report: Present-day ozone distribution and trends relevant to human health. Elem Sci Anth 6(1), 12. DOI: https://doi.org/10.1525/elementa.273.

Fowler, D., Pilegaard, K., Sutton, M.A., Ambus, P., Raivonen, M., Duyzer, J., Simpson, D., Fagerli, H., Fuzzi, S., Schjoerring, J.K., Granier, C., Neftel, A., Isaksen, I.S.A., Laj, P., Maione, M., Monks, P.S., Burkhardt, J., Daemmgen, U., Neirynck, J., Personne, E., Wichink-Kruit, R., et al., 2009. Atmospheric composition change: Ecosystems-Atmosphere interactions. Atmos. Environ. 43, 5193–5267. https://doi.org/10.1016/j.atmosenv.2009.07.068.

Gangoiti, G., Alonso, L., Navazo, M., Albizuri, A., Perez-Landa, G., Matabuena, M., Valdenebro, V., Maruri, M., García, J.A., Millán, M.M., 2002. Regional transport of pollutants over the Bay of Biscay: analysis of an ozone episode under a blocking anticyclone in west-central Europe. Atmos. Environ. 36, 8, 1349–1361. https://doi.org/10.1016/S1352-2310(01)00536-2.

Gangoiti, G., Albizuri, A., Alonso, L., Navazo, M., Matabuena, M., Valdenebro, V., García, J.A., Millán, M.M., 2006. Sub-continental transport mechanisms and pathways during two ozone episodes in northern Spain. Atmos. Chem. Phys. 6, 1469–1484.

Gangoiti, G., Millán, M.M., Salvador, R., Mantilla, E., 2001. Long-range transport and re-circulation of pollutants in the western Mediterranean during the project Regional Cycles of Air Pollution in the West-Central Mediterranean Area, Atmospheric Environment, 35, 6267-6276, 10.1016/S1352-2310(01)00440-X.

GBD: Global Burden of Disease Study 2016 Cause-Specific Mortality 1980–2016, Seattle, United States: Institute for Health Metrics and Evaluation (IHME), 2016.

Hersbach, H., Bell, B., Berrisford, P., Biavati, G., Horányi, A., Muñoz Sabater, J., Nicolas, J., Peubey, C., Radu, R., Rozum, I., Schepers, D., Simmons, A., Soci, C., Dee, D., Thépaut, J-N., 2019. ERA5 monthly averaged data on single levels from 1959 to present. Copernicus Climate Change Service (C3S) Climate Data Store (CDS). 10.24381/cds.f17050d7.

HTAP: Task Force on Hemispheric Transport of Air Pollution, 2010. Hemispheric Transport of Air Pollution 2010, Part A: Ozone and Particulate Matter, United Nations, New York and Geneva, 2010.

In 't Veld, M., Carnerero, C., Massagué, J., Alastuey, A., de la Rosa, J., Sánchez, A.M., Escudero, M., Mantilla, E., Gangoiti, G., Pérez, C. Olid, M., Moreta, J.R., Hernández, J.L., Santamaría, J. Millán, M., Querol, X., 2021. Understanding the local and remote source contributions to ambient O3 during a pollution episode using a combination of experimental approaches in the Guadalquivir Valley, Southern Spain. Sci. Total Environ. 777. 144579. 10.1016/j.scitotenv.2020.144579.

IPCC: AR6 Climate Change 2021: The Physical Science Basis. Intergovernmental Panel of Climate Change, United Nations, Full Report. 3946 pp, https://www.ipcc.ch/report/ar6/wg1/downloads/report/IPCC_AR6_WGI_Full_Report.pdf, last access: 5 April 2022, 2021.

Jacob, D., Winner, D., 2009. Effect of climate change on air quality. Atmos. Environ. 43 (1), 51–63.

Kalabokas, P., Hjorth, J., Foret, G., Dufour, G., Eremenko, M., Siour, G., Cuesta, J., Beekmann, M., 2017. An investigation on the origin of regional springtime ozone episodes in the western Mediterranean. Atmos. Chem. Phys. 17, 3905–3928. https://doi.org/10.5194/acp-17-3905-2017.

Lefohn, A.S., Malley, C.S., Simon, H., Wells, B., Xu, X., et al., 2017. Responses of human health and vegetation exposure metrics to changes in ozone concentration distributions in the European Union, United States, and China. Atmos. Environ 152, 123–145. https://doi.org/10.1016/j.atmosenv.2016.12.025.

Lefohn, A.S., Malley, C.S., Smith, L., Wells, B., Hazucha, M., Simon, H., Naik, V., Mills, G., Schultz, M.G., et al., 2018. Tropospheric Ozone Assessment Report: Global ozone metrics for climate change, human health, and crop/ecosystem research. Elem Sci Anth 6, 28. DOI: https://doi. org/10.1525/elementa.279.

Massagué, J., Carnerero, C., Escudero, M., Baldasano, J. M., Alastuey, A., Querol, X., 2019. 2005–2017 ozone trends and potential benefits of local measures as deduced from air quality measurements in the north of the Barcelona metropolitan area, Atmos. Chem. Phys., 19, 7445–7465, 10.5194/acp-19-7445-2019.

Massagué, J., Contreras, A., Campos, A., Alastuey, A., Querol, X., 2021. 2005–2018 trends in ozone peak concentrations and spatial contributions in the Guadalquivir Valley, Southern Spain. Atmospheric Environment 254, 22, 118385. 10.1016/j.atmosenv.2021.118385.

McLinden, C.A., Olsen, S.C., Hannegan, B., Wild, O., Prather, M.J., Sundet, J., 2000. Stratospheric ozone in 3-D models: A simple chemistry and the cross-tropopause flux. J. Geophys. Res. Atmos. 105, 14653–14665. https://doi.org/10.1029/2000jd900124.

Millán, M.M., Salvador, R., Mantilla, E., Kallos, G., 1997. Photooxidant dynamics in the Mediterranean basin in summer: Results from European research projects. J. Geophys. Res. 102, 8811–8823.

Millán, M.M., Mantilla, E., Salvador, R., Carratalá, A., Sanz, M.J., Alonso, L., Gangoiti, G., Navazo, M., 2000. Ozone Cycles in the Western Mediterranean Basin: Interpretation of Monitoring Data in Complex Coastal Terrain. J. Appl. Meteorol. 39, 487–508.

Millán, M.M., Sanz, M.J., Salvador, R., Mantilla, E., 2002. Atmospheric dynamics and ozone cycles related to nitrogen deposition in the western Mediterranean. Environ. Pollut. 118, 167–186.

Millán M.M., 2009. El ozono troposférico en el sur de Europa: aspectos dinámicos documentados en proyectos europeos, CEAM Report for the Ministry of Agriculture, Food and Environment, INF FIN/O3/2009 (annex), 156 pp.

Millán, M.M., 2014. Extreme hydrometeorological events and climate change predictions in Europe, J. Hydrol., 518B, 206–224.

Mills, G., Pleijel, H., Malley, C., Sinha, B., Cooper, O. R., Schultz, M. G., Neufeld, H. S., Simpson, D., Sharps, K., Feng, Z.,Gerosa, G., Harmens, H., Kobayashi, K., Saxena, P., Paoletti, E., Sinha, V., Xu, X., Helmig, D., Lewis, A., 2018. Tropospheric Ozone Assessment Report: Present-day tropospheric ozone distribution and trends relevant to vegetation. Science of the Anthropocene, 6, 47, 10.1525/elementa.302.

Monks, P.S., Archibald, A.T., Colette, A., Cooper, O., Coyle, M., Derwent, R., Fowler, D., Granier, C., Law, K.S., Mills, G.E., Stevenson, D.S., Tarasova, O., Thouret, V., von Schneidemesser, E., Sommariva, R., Wild, O., Williams, M.L., 2015. Tropospheric ozone and its precursors from the urban to the global scale from air quality to short-lived climate forcer. Atmos. Chem. Phys. 15, 8889–8973.

Monteiro, A., Strunk, A., Carvalho, A., Tchepel, O., Miranda, A.I., Borrego, C., Saavedra, S., Rodríguez, A., Souto, J., Casares, J., Friese, E., Elbern, H., 2012. Investigating a high ozone episode in a rural mountain site. Environ. Pollut. 162, 176–189. https://doi.org/10.1016/j.envpol.2011.11.008.

Myhre, G., Shindell, D., Bréon, F.M., Collins, W., Fuglestvedt, J., Huang, J., Koch, D., Lamarque, J.F., 794 Lee, D., Mendoza, B., Nakajima, T., 2013. Climate change 2013: the physical science basis. Contribution 795 of Working Group I to the Fifth Assessment Report of the Intergovernmental Panel on Climate 796 Change. K., Tignor, M., Allen, SK, Boschung, J., Nauels, A., Xia, Y., Bex, V., and Midgley, PM, 797 Cambridge University Press Cambridge, United Kingdom and New York, NY, USA.

Notario, A., Bravo, I., Adame, J.A., Díaz-de-Mera, Y., Aranda, A., Rodríguez, A., Rodríguez, D., 2012. Analysis of NO, NO2, NOx, O3 and oxidant (Ox=O3+NO2) levels measured in a metropolitan area in the southwest of Iberian Peninsula. Atmos. Res. 104–105 (2), 217–226. https://doi.org/10.1016/j.atmosres.2011.10.008.

Notario, A., Bravo, I., Adame, J.A., et al., 2013. Behaviour and variability of local and regional oxidant levels ($OX = O_3 + NO_2$) measured in a polluted area in central-southern of Iberian Peninsula. Environ Sci Pollut Res 20, 188–200. https://doi.org/10.1007/s11356-012-0974-1, 2013.

Olson, J.R., Crawford, J.H., Davis, D.D., Chen, G., Avery, M.A., Barrick, J.D.W., Sachse, G.W., Vay, S.A., Sandholm, S.T., Tan, D., Brune, W.H., Faloona, I.C., Heikes, B.G., Shetter, R.E., Lefer, B.L., Singh, H.B., Talbot, R.W., Blake, D.R., 2001. Seasonal differences in the photochemistry of the South Pacific: A comparison of observations and model results from PEM-Tropics A and B. J. Geophys. Res. 106, 32749–32766.

Otero, N., Sillmann, J., Schnell, J.L., Rust, H.W., Butler, T., 2016. Synoptic and meteorological drivers of extreme ozone concentrations over Europe. Environ. Res. Lett. 11, 24005. https://doi.org/10.1088/1748-9326/11/2/024005.

Paoletti, E., De Marco, A., Beddows, D.C.S., Harrison, R.M., Manning, W., 2014. J.: Ozone levels in European and USA cities are increasing more than at rural sites, while peak values are decreasing. Environ. Pollut. 192, 295–299. https://doi.org/10.1016/j.envpol.2014.04.040.

Pay, M.T., Gangoiti, G., Guevara, M., Napelenok, S., Querol, X., Jorba, O., García-Pando, P., 2019. C.: Ozone source apportionment during peak summer events over southwestern Europe. Atmos. Chem. Phys. 19, 5467–5494. https://doi.org/10.5194/acp-19-5467-2019.

Plaza, J., Pujadas, M., Artíñano, B., 1997. Formation and Transport of the Madrid Ozone Plume. JAPCA J. Air Waste Ma. 47, 766–774.

Querol, X., Alastuey, A., Pandolfi, M., Reche, C., Perez, N., Minguillon, M.C., Moreno, T., Viana, M., Escudero, M., Orio, A., Pallares, M., Reina, F., 2014. 2001–2012 trends on air quality in Spain Sci. Total Environ. 490, 957–969.

Querol, X., Alastuey, A., Orio, A., Pallares, M., Reina, F., Dieguez, J.J., Mantilla, E., Escudero, M., Alonso, L., Gangoiti, G., Millán, M., 2016. On the origin of the highest ozone episodes in Spain. Sci. Total Environ. 572, 379–389.

Querol, X., Gangoiti, G., Mantilla, E., Alastuey, A., Minguillón, M.C., Amato, F., Reche, C., Viana, M., Moreno, T., Karanasiou, A., Rivas, I., Pérez, N., Ripoll, A., Brines, M., Ealo, M., Pandolfi, M., Lee, H.-K., Eun, H.-R., Park, Y.-H., Escudero, M., Beddows, D., Harrison, R.M., Bertrand, A., Marchand, N., Lyasota, A., Codina, B., Olid, M., Udina, M., Jiménez-Esteve, B., Soler, M.R., Alonso, L., Millán, M., Ahn, K.-H., 2017. Phenomenology of high-ozone episodes in NE Spain. Atmos. Chem. Phys. 17, 2817–2838.

Querol, X., Alastuey, A., Gangoiti, G., Perez, N., Lee, H.K., Eun, H.R., Park, Y., Mantilla, E., Escudero, M., Titos, G., Alonso, L., Temime-Roussel, B., Marchand, N., Moreta, J.R., Revuelta, M.A., Salvador, P., Artíñano, B., García dos Santos, S., Anguas, M., Notario, A., Saiz-Lopez, A., Harrison, R.M., Millán, M., Ahn, K.-H., 2018. Phenomenology of summer ozone episodes over the Madrid Metropolitan Area, central Spain. Atmos. Chem. Phys. 18, 6511–6533. https://doi.org/10.5194/acp-18-6511-2018.

R Core Team: R: A Language and environment for Statistical Computing. R Foundation for Statistical Computing. Vienna, Austria. https://www.R-project.org, last access: 5 April 2022, 2021.

Reche, C., Moreno, T., Amato, F., Pandolfi, M., Pérez, J., de la Paz, D., Diaz, E., Gómez-Moreno, F.J., Pujadas, M., Artíñano, B., Reina, F., Orio, A., Pallarés, M., Escudero, M., Tapia, O., Crespo, E., Vargas, R., Alastuey, A., X., 2018. Querol.: Spatio-temporal patterns of high summer ozone events in the Madrid Basin, Central Spain. Atmos. Environ. 185, 207–220. http://www.sciencedirect.com/science/article/pii/S1352231018302991,.

Saavedra, S. Rodríguez, A., Taboada, J. J., Souto, J. A., Souto, J. A., Synoptic patterns and air mass transport during ozone episodes in northwestern Iberia. Science of the Total Environment, 97-110, 10.1016/j.scitotenv.2012.09.014, 2012.

Saiz-Lopez, A., Adame, J.A., Notario, A., Poblete, J., Bolívar, J.P., Albaladejo, J., 2009. Year-Round Observations of NO, NO2, O3, SO2, and Toluene Measured with a DOAS System in the Industrial Area of Puertollano, Spain. Water Air Soil Pollut 200, 277–288. https://doi.org/10.1007/s11270-008-9912-8, 2009.

Santurtún, A., González-Hidalgo, J.C., Sanchez-Lorenzo, A., Zarrabeitia, M.T., 2015. Surface ozone concentration trends and its relationship with weather types in Spain (2001–2010), Atmospheric Environment, Volume 101, 2015, Pages 10-22, ISSN 1352-2310, 10.1016/j.atmosenv.2014.11.005.

Schultz, M.G., Schroeder, S., Lyapina, O., Cooper, O.S., et al., 2017. Tropospheric Ozone Assessment Report: Database and metrics data of global surface ozone observations. Elem Sci Anth 5: 58, 26.

Seco, R., Peñuelas, J., Filella, I., Llusià, J., Molowny-Horas, R., Schallhart, S., Metzger, A., Müller, M., Hansel, A., 2011. Contrasting winter and summer VOC mixing ratios at a forest site in the Western Mediterranean Basin: the effect of local biogenic emissions, Atmos. Chem. Phys., 11, 13161–13179, 10.5194/acp-11-13161-2011.

Sen, P.K., 1968. Estimates of regression coefficient based on Kendall's tau. J. Am. Stat. Assoc. 63 (324).

Sicard, P., De Marco, A., Troussier, F., Renou, C., Vas, N., Paoletti, E., 2013. Decrease in surface ozone concentrations at Mediterranean remote sites and increase in the cities. Atmos. Environ. 79, 705–715.

Sicard, P., Serra, R., Rossello, P., 2016. Spatio-temporal trends of surface ozone concentrations and metrics in France. Environ Res 149, 122–144. https://doi.org/10.1016/j.envres.2016.05.014, 2016.

Sicard, P., Agathokleous, E., Araminiene, V., Carrari, E., Hoshika, Y., De Marco, A., Paoletti, E., 2018. Should we see urban trees as effective solutions to reduce increasing ozone levels in cities? Environ Pollut 2018 (243), 163–176.

Sicard, P., Paoletti, E., Agathokleous, E., Araminien_e, V., Proietti, C., et al., 2020. Ozone weekend effect in cities: deep insights for urban air pollution control. Environ Res 191, 110193.

Sicard, 2021. Ground-level ozone over time: An observation-based global overview. Current Opinion in Environmental Science & Health, Volume 19, 2021, 100226, ISSN 2468-5844, 10.1016/j.coesh.2020.100226.

Simon, H., Reff, A., Wells, B., Xing, J., Frank, N., 2015. Ozone Trends Across the United States over a Period of Decreasing NOx and VOC Emissions. Environ. Sci. Technol 49, 186–195. https://doi.org/10.1021/es504514z.

Sokhi, R.S., Singh, V., Querol, X., et al., 2021. A global observational analysis to understand changes in air quality during exceptionally low anthropogenic emission conditions. Environ. Int. 157, 106818 https://doi.org/10.1016/j.envint.2021.106818.

Solberg, S., Bergström, R., Langner, J., Laurila, T., Lindskog, A., 2005. Changes in Nordic surface ozone episodes due to European emission reductions in the1990s. Atmos. Environ. 39, 179–192.

Stevenson, D.S., Dentener, F.J., Schultz, M.G., Ellingsen, K., van Noije, T.P.C., Wild, O., Zeng, G., Amann, M., Atherton, C.S., Bell, N., Bergmann, D.J., Bey, I., Butler, T., Cofala, J., Collins, W.J., Derwent, R.G., Doherty, R.M., Drevet, J., Eskes, H.J., Fiore, A.M., Gauss, M., et al., 2006. Multimodel ensemble simulations of present-day and near-future tropospheric ozone. J. Geophys. Res. Atmos. 111, D08301 https://doi.org/10.1029/2005jd006338.

Tapia, O., Escudero, M., Lozano, A., Anzano, J., Mantilla, E., 2016. New classification scheme for ozone monitoring stations based on frequency distribution of hourly data. Sci. Total Environ. 544, 1–9. https://doi.org/10.1016/j.scitotenv.2015.11.081, 2016.

Theil, H., 1950. A rank invariant method of linear and polynomial regression analysis, i, ii, iii, Proceedings of the Koninklijke Nederlandse Akademie Wetenschappen, Series A - Mathematical Sciences 53, 386-392, 521-525, 1397-1412.

UNECE, United Nations Economic Commission for Europe. Convention on Long-Range Trans-boundary Air Pollution. Mapping Critical Levels for Vege-tation. International Cooperative Programme on Effects of Air Pollution on Natural Vegetation and Crops. Bangor, UK, 2010.

von Schneidemesser, E., Monks, P.S., Allan, J.D., Bruhwiler, L., Forster, P., et al., 2015. Chemistry and the linkages between air quality and climate change. Chem. Rev 115 (10), 3856–3897. https://doi.org/10.1021/acs.chemrev.5b00089.

Wei, J., Li, Z., Dickerson, R., Pinker, R., Wang, J., Liu, X., Sun, L., Xue, W., Cribb, M., 2022. Full-coverage mapping and spatiotemporal variations of ground-level ozone (O3) pollution from 2013 to 2020 across China. Remote Sens. Environ. 270, 112775 https://doi.org/10.1016/j.rse.2021.112775, 2022.

WHO: Air quality guidelines for particulate matter, ozone, nitrogen dioxide and sulfur dioxide. Global update 2005. https://apps.who.int/iris/handle/10665/69477, last access: 5 April 2022, 2006.

WHO Regional Office for Europe: Review of evidence on health aspects of air pollution—REVIHAAP project: technical report, WHO Regional Office for Europe, Copenhagen 302 pp., http://www.euro.who.int/_data/assets/pdf_file/0004/193108/REVIHAAP-Final-technical-report-final-version.pdf?ua=1, last access: 5 April 2022, 2013a.

WHO Regional Office for Europe: Health Risks of Air Pollution in Europe–HRAPIE Project: Recommendations for Concentration-Response Functions for Cost–Benefit Analysis of Particulate Matter, Ozone and Nitrogen Dioxide, Copenhagen, 65 pp., available at: http://www.euro.who.int/_data/assets/pdf_file/0017/234026/e96933.pdf?ua=1 (last access: 5 April 2022), 2013b.

WHO global air quality guidelines. Particulate matter (PM2.5 and PM10), ozone, nitrogen dioxide, sulfur dioxide and carbon monoxide. Geneva: World Health Organization; https://apps.who.int/iris/handle/10665/345329, last access: 5 April 2022, 2021.

Wilson, R.C., Fleming, Z.L., Monks, P.S., Clain, G., Henne, S., et al., 2012. Have primary emission reduction measures reduced ozone across Europe? An analysis of European rural background ozone trends 1996–2005.Atmos. Chem Phys 12, 437–454.

Yan, Y., Lin, J., Pozzer, A., Kong, S., Lelieveld, J., 2019. Trend reversal from high-to-low and from rural-to-urban ozone concentrations over Europe. Atmos Environ. 213, 25–36.

Young, P.J., Archibald, A.T., Bowman, K.W., Lamarque, J.-F., Naik, V., Stevenson, D.S., Tilmes, S., Voulgarakis, A., Wild, O., Bergmann, D., Cameron-Smith, P., Cionni, I., Collins, W.J., Dalsøren, S.B., Doherty, R.M., Eyring, V., Faluvegi, G., Horowitz, L.W., Josse, B., Lee, Y.H., et al., 2013. Preindustrial to end 21st century projections of tropospheric ozone from the Atmospheric Chemistry and Climate Model Intercomparison Project (ACCMIP). Atmos. Chem. Phys. 13, 2063–2090. https://doi.org/10.5194/acp-13-2063-2013.

Further reading

Gaudel, A., Cooper, O.R., Ancellet, G., et al.: Tropospheric Ozone Assessment Report: Present-day distribution and trends of tropospheric ozone relevant to climate and global atmospheric chemistry model evaluation. Elementa: Sci. Anthropocene 1 January 2018; 6 39. doi: 10.1525/elementa.291.